https://doi.org/10.5194/bg-2020-24
Preprint. Discussion started: 29 January 2020


Biogeosciences Discussions

# The impact of intertidal areas on the carbonate system of the southern North Sea

Fabian Schwichtenberg[1], Johannes Pätsch[1,5], Michael Ernst Böttcher[2,3,4], Helmuth Thomas[5], Vera Winde[2], Kay-Christian Emeis[5]

[1] Theoretical Oceanography, University Hamburg, D-20146 Hamburg, Bundesstr. 53, Germany

[2] Geochemistry & Isotope Biogeochemistry Group, Department of Marine Geology, Leibniz Institute of Baltic Sea Research (IOW), Seestr. 15, D-18119 Warnemünde, Germany

[3] Marine Geochemistry, University of Greifswald, Friedrich-Ludwig-Jahn Str. 17a, D-17489 Greifswald, Germany

[4] Department of Maritime Systems, Interdisciplinary Faculty, University of Rostock, Albert.Enistein-Straße 21, D-18059 Rostock, Germany

[5] Institute of Coastal Research, Helmholtz Zentrum Geesthacht (HZG), Max-Planck.Str. 1, D-21502 Geesthacht, Germany

Correspondence to Johannes Pätsch (johannes.paetsch@uni-hamburg.de)

**Abstract**

The coastal ocean is strongly affected by ocean acidification because it is shallow and has a low volume. Earlier observations of dissolved inorganic carbon (DIC) and total alkalinity (TA) in the southern part of the North Sea and the German Bight, a Northwest-European shelf sea, have revealed lower acidification effects than expected. It has been assumed that anaerobic degradation and subsequent TA release in the adjacent tidal areas ('Wadden Sea') in summer time is responsible for this phenomenon. In this study the exchange rates of TA and DIC between the Wadden Sea and the North Sea and the consequences for the carbonate system in the German Bight are estimated using a 3-D ecosystem model. Observed TA and DIC sources in the Wadden Sea were considered as boundary conditions. This procedure is based on the dynamic behaviour of the Wadden Sea as an area of effective production and decomposition of organic material. In addition, modelled tidal water mass exchange was used to transport

https://doi.org/10.5194/bg-2020-24
Preprint. Discussion started: 29 January 2020




material between the open North Sea and the Wadden Sea. In the model, 39 Gmol TA $yr^{-1}$ were exported from the Wadden Sea into the North Sea, which is lower than a previous estimate, but within a comparable range. Furthermore, the interannual variabilities of TA and DIC concentrations, which were mainly driven by hydrodynamic conditions, were examined for the years 2001 – 2009. Variability in the carbonate system of the German Bight is related to weather in that the occurrence of weak meteorological blocking situations leads to enhanced accumulation of TA there. The results suggest that the Wadden Sea is an important driver of the carbonate system variability in the southern North Sea. According to the model results, on average 63 % of all TA mass changes in the German Bight were caused by net transport, 25 % by Wadden Sea export, 9 % were caused by the internal production of TA and 3 % caused by effective TA river loads (i.e. river load including freshwater dilution). The ratio of exported TA and DIC reflects the dominant underlying biogeochemical processes in the different Wadden Sea areas. Aerobic degradation of organic matter plays a key role in the North Frisian Wadden Sea during all seasons of the year. In the East Frisian Wadden Sea anaerobic degradation of organic matter dominated.

## 1. Introduction

Shelf seas are highly productive areas constituting the interface between the inhabited coastal areas and the global ocean. Although they represent only 7.6% of the world ocean's area, current estimates assume that they contribute approximately 21% of total global ocean $CO_2$ sequestration (Borges, 2011). At the global scale the uncertainties of these estimates are significant due to the lack of spatially and temporally resolved field data. Some studies investigated regional carbon cycles in regional detail (e.g., Kempe & Pegler, 1991; Brasse et al., 1999; Reimer et al., 1999; Thomas et al., 2004; 2009; Artioli et al., 2012; Lorkowski et al., 2012; Burt et al., 2016; Shadwick et al., 2011; Laruelle et al., 2014; Carvalho et al., 2017) and pointed out sources of uncertainties specifically for coastal settings. For example pH variations in coastal- and shelf regions can be up to an order of magnitude higher than in the open ocean (Provoost et al, 2010). The nearshore effects of $CO_2$ uptake and acidification are difficult to determine, because of the shallow water depth and a possible superposition by benthic-pelagic coupling. Strong variations in fluxes of TA are associated with inflow of nutrients from rivers, submarine groundwater discharge (SGD) and

https://doi.org/10.5194/bg-2020-24
Preprint. Discussion started: 29 January 2020


from benthic-pelagic pore water exchange (e.g., Billerbeck et al., 2006; Riedel et al., 2010; Moore et al., 2011; Winde et al., 2014; Santos et al., 2012; 2015; Brenner et al., 2016; Burt et al., 2014, 2016; Seibert et al., 2019).

Berner et al. (1970) were one of the first who investigated elevated TA in anoxic pore water sediments caused by microbial dissimilatory sulphate reduction. Further studies were conducted, for instance, at the Californian coast (Dollar et al., 1991; Smith & Hollibaugh, 1993; Chambers et al., 1994). There, the observed enhanced TA export from sediments was related to the burial of reduced sulphur compounds (pyrite). Other studies conducted in the Satilla and Altamaha estuaries and the adjacent continental shelf found non-conservative mixing lines of TA versus salinity, which was attributed to anaerobic TA production in nearshore sediments (Wang & Cai, 2004; Cai et al., 2010).

The focus of the present study is the southern part of the North Sea located on the Northwest European Shelf. This shallow part of the North Sea is connected with the tidal areas of the Wadden Sea via deep channels between barrier islands enabling an exchange of water and dissolved and suspended material (Rullkötter, 2009; Lettmann et al., 2009; Kohlmeier and Ebenhöh, 2009). The Wadden Sea extends from Den Helder (Netherland) in the west to Esbjerg (Denmark) in the north covering an area of about 9500 $km^2$ (Ehlers, 1994). The entire system is characterised by semidiurnal tides with a tidal range between 1.5 m in the most westerly part and 4 m in the estuaries of the rivers Weser and Elbe (Streif, 1990).

In comparison to the central and northern part of the North Sea, TA concentrations in the southern part are significantly elevated during summer (Salt et al., 2013; Thomas et al., 2009). The observed high TA concentrations have been attributed to an impact from the adjacent tidal areas (Hoppema, 1990; Kempe & Pegler, 1991; Brasse et al., 1999; Reimer et al., 1999; Thomas et al., 2009; Winde et al., 2014). Using several assumptions, Thomas et al. (2009) calculated an annual TA export from the Wadden Sea / Southern Bight of 73 Gmol TA $yr^{-1}$ to close the TA budget for the entire North Sea.

Additional data of river input, of anaerobic TA production in the Wadden Sea and nitrogen deposition in combination with a 3-D model system permit us to refine the budget terms and

https://doi.org/10.5194/bg-2020-24
Preprint. Discussion started: 29 January 2020


replace the original closing term with data. The new results are discussed on the background of the budgeting assumptions of Thomas et al. (2009).

## 2. Methods

### *2.1. Model domain and validation area*

The model domain (Fig. 1) was first applied by Pätsch et al. (2010). For model validations (green: validation area, Fig. 1), an area was chosen that includes the German Bight as well as parts of the Danish and the Dutch coast. The western boundary of the validation area is situated at 4.5° E. The southern and northern boundaries are at 53.5° and 55.5° N, respectively. For the calculation of box averages of DIC and TA a bias towards the deeper areas with more volume should be avoided. Therefore, each water column (having data) within the validation area delivered one mean value, which is calculated by volume-weighted vertical averaging. In the case of sparse observational data, which cluster towards the coast, these mean water column averages were horizontally interpolated onto the model grid. After this procedure, area-weighted average box values were calculated. In case of box-averaging model output, the same procedure was applied, but without horizontal interpolation.

### *2.2. The hydrodynamic module*

The physical parameters temperature, salinity, horizontal and vertical advection as well as turbulent mixing were calculated by the submodule HAMSOM (Backhaus, 1985), which was integrated in the ECOHAM model. Details are described by Backhaus & Hainbucher (1987) and Pohlmann (1996). The hydrodynamic model ran prior to the biogeochemical part. Daily result fields were stored for driving the biogeochemical model in offline mode. Surface elevation, temperature and salinity resulting from the Northwest European Shelf model application (Lorkowski et al., 2012) were used as boundary conditions at the southern and northern boundaries. The temperature of the shelf run by Lorkowski et al. (2012) showed a constant offset compared with observations (their Fig. 3), because incoming solar radiation was calculated too high. For the present simulations the shelf run has been repeated with adequate solar radiation forcing.

https://doi.org/10.5194/bg-2020-24
Preprint. Discussion started: 29 January 2020


River-induced horizontal transport due to the hydraulic gradient is incorporated (Große et al., 2017; Kerimoglu et al., 2018). This component of the hydrodynamic horizontal transport corresponds to the amount of freshwater discharge.

### *2.3. Freshwater discharge*

Daily data of freshwater fluxes from 16 rivers were used (Fig. 1). For the German Bight and the other continental rivers daily observations of runoff provided by Pätsch & Lenhart (2008) were incorporated. The discharges of the rivers Elbe, Weser and Ems were increased by 21%, 19% and 30% in order to take additional drainage into account that originated from the area downstream of the respective points of observation (Radach and Pätsch, 2007). The respective tracer loads were increased accordingly. The data of Neal (2002) were implemented for the British rivers for all years with daily values for freshwater. The annual amounts of freshwater of the different rivers are shown in the appendix (Table A1). Riverine freshwater discharge was also considered for the calculation of the concentrations of all biogeochemical tracers in the model.

### *2.4. Meteorological forcing*

The meteorological forcing was provided by NCEP Reanalysis (Kalnay et al., 1996) and interpolated on the model grid field. It consisted of six-hourly fields of air temperature, relative humidity, cloud coverage, wind speed, atmospheric pressure, and wind stress for every year. 2-hourly and daily mean short wave radiation were calculated from astronomic insolation and cloudiness with an improved formula (Lorkowski et al., 2012).

### *2.5. The biogeochemical module*

The relevant biogeochemical processes and their parameterisations have been detailed in Lorkowski et al. (2012). In former model setups TA was restored to prescribed values derived from observations (Thomas et al., 2009) with a relaxation time of two weeks (Kühn et al., 2010; Lorkowski et al., 2012). The changes in TA treatment for the study at hand is described below. Results from the Northwest European Shelf model application (Lorkowski et al., 2012) were used as boundary conditions for the recent biogeochemical simulations at the southern and northern boundaries (Fig. 1).

https://doi.org/10.5194/bg-2020-24
Preprint. Discussion started: 29 January 2020


147

148 ***2.6. River input***

149 **2.6.1. Data sources**

150 River load data for the main continental rivers were taken from the report by Pätsch &
151 Lenhart (2008) that was kept up to date continuously so that data for the years 2007 – 2009
152 were also available (https://wiki.cen.uni-hamburg.de/ifm/ECOHAM/DATA_RIVER). They
153 calculated daily loads of nutrients and organic matter based on data provided by the
154 different river authorities. Additionally, loads of the River Eider were calculated according to
155 Johannsen et al. (2008).

156 Up to now, all ECOHAM applications used constant riverine DIC concentrations. TA was not
157 used. For the study at hand we introduced time varying riverine TA and DIC concentrations.
158 New data of freshwater discharge were introduced, as well as TA and DIC loads for the
159 British rivers (Neal, 2002). Monthly mean concentrations of TA and DIC were added for the
160 Dutch rivers (www.waterbase.nl) and for the German river Elbe (Amann et al., 2015).

161 The data sources and positions of the river mouths of all 16 rivers are shown in Table A2 and
162 in Fig. 1. The respective riverine concentrations of TA and DIC are given in Table A3.
163 Schwichtenberg (2013) describes the river data in detail.

164 A few small flood gates ("Siel") and rivers transport fresh water from the recharge areas into
165 the intertidal areas (Streif, 1990). The recharge areas for these inlets differ considerably
166 from each other, leading to different relative contributions for the fresh water input.
167 Whereas the Schweiburger Siel (22.2 $km^2$) and the Hooksieler Binnentief are only of minor
168 importance, the Vareler Siel, the Eckenwarder Siel, and the Maade Siel are of medium
169 importance, and the highest contribution may originate from the Wangersiel, the Dangaster
170 Siel, and the Jade-Wapeler Siel (Lipinski, 1999).

171 **2.6.2. Effective river input**

172 In order to analyse the net effect of river input, the effective river input ($Riv_{eff}$) is introduced:

173

$$Riv_{eff} = \frac{\Delta C|_{riv}}{yr} \cdot V \qquad (1)$$

174

https://doi.org/10.5194/bg-2020-24
Preprint. Discussion started: 29 January 2020


175 with $\Delta C|_{riv}$: the concentration change in the river mouth cell due to river load *riv* and the
176 freshwater flux from the river. *V* is the volume of the river mouth cell.

177

178 ***2.7. Sampling of DIC and TA***

179 DIC and TA concentrations for selected freshwater inlets sampled in October 2010 and May
180 2011 are presented in Table 6. Sampling and analyses took place as described by Winde et
181 al. (2014) and are here reported for completeness only. The data are deposited in the data
182 base https://www.pangaea.de. The samples for TA measurements were filled without
183 headspace into pre-cleaned Exetainer®, filled with 0.1ml saturated $HgCl_2$ solution. The
184 samples for DIC analysis were completely filled into ground-glass-stoppered bottles, and
185 then poisoned with saturated $HgCl_2$ solution. The DIC concentrations were determined at
186 IOW by coulometric titration according to Johnson et al. (1993), using reference material
187 provided by A. Dickson (University of California, San Diego; Dickson et al., 2003) for the
188 calibration. TA was measured by potentiometric titration using HCl using a Schott titri plus
189 equipped with an IOline electrode A157.

190 ***2.8. Concept of Alkalinity and the carbonate system***

191 The main extension in the present study was the introduction of a prognostic treatment of
192 TA (Pätsch et al., 2018) in order to study the impact of biogeochemical and physical changes
193 of TA onto the carbonate system and especially on acidification. The physical part contained
194 advective and mixing processes as well as dilution by riverine freshwater input. The
195 biogeochemical part was driven by formation and dissolution of calcite, nutrient dynamics
196 and also by atmospheric deposition of reduced and oxidised nitrogen. The theoretical
197 background to this has been outlined by Wolf-Gladrow et al. (2007).

198 ***2.9. Implementation of Wadden Sea dynamics***

199 For the present study the exchange of TA and DIC between North Sea and Wadden Sea was
200 implemented into the model by defining sinks and sources of TA and DIC for some of the
201 south-eastern cells of the North Sea grid (Fig. 1). The cells with adjacent Wadden Sea were
202 separated into three exchange areas: The East Frisian and the North Frisian Wadden Sea as
203 well as the Jade Bay, distinguished by “E”, “N” and “J” (Fig. 1, right side).

https://doi.org/10.5194/bg-2020-24
Preprint. Discussion started: 29 January 2020




Two parameters were determined in order to quantify the TA and DIC exchange between the Wadden Sea and the North Sea.

1. Concentration changes of pelagic TA and DIC in the Wadden Sea during one tide, and
2. Water mass exchange between the back-barrier islands and the open sea during one tide

Measured concentrations of TA and DIC (Winde, 2013; Winde et al., 2014) as well as modelled water mass exchange rates of the export areas by Grashorn (2015) served as basis for the calculated exchange. Details on flux calculations and measurements are described below. The daily Wadden Sea exchange of TA and DIC was calculated as:

$$wad\_flu = \frac{wad\_sta * wad\_exc}{vol} \quad (2)$$

Differences in measured concentrations in the Wadden Sea during rising and falling water levels were temporally interpolated and summarized as *wad_sta* [mmol $m^{-3}$]. Modelled daily Wadden Sea exchange rates of water masses (tidal prisms during falling water level) were defined as *wad_exc* [$m^3$ $d^{-1}$], and the volume of the corresponding North Sea grid cell was *vol* [$m^3$]. *wad_flu* [mmol $m^{-3}$ $d^{-1}$] were the daily concentration changes of TA and DIC in the respective North Sea grid cells.

In fact, some amounts of the tidal prisms return without mixing with North Sea water, and calculations of Wadden Sea – North Sea exchange should therefore consider flushing times in the respective back-barrier areas. Since differences in measured concentrations between rising and falling water levels were used, this effect is already assumed to be represented in the data. This approach enabled the use of tidal prisms without consideration of any flushing times.

https://doi.org/10.5194/bg-2020-24
Preprint. Discussion started: 29 January 2020


#### 2.9.1. Wadden Sea - measurements

The flux calculations for the Wadden Sea – North Sea exchange were carried out representatively in tidal basins of the East and North Frisian Wadden Sea (Spiekeroog Island, Sylt-Rømø) as well as in the Jade Bay. For the present study seawater samples were used on tidal cycles during different seasons (Winde, 2013). The mean concentrations of TA and DIC during rising and falling water levels and the respective differences (ΔTA and ΔDIC) are given in Table 1. Measurements in August 2002 were taken from Moore et al. (2011). The Δ-values were used as *wad_sta* and linearly interpolated between the times of observations for the simulations. Of course, the linear progress of the Δ-values did not represent the natural behaviour perfectly, especially if only few data are available. As a consequence, possible short events of high TA and DIC export rates that occurred in periods outside the observation periods may have been missed.

A statistical analysis of uncertainties of ΔTA and ΔDIC was not possible, because concentrations were measured with a lag of 2 hours after low tide and high tide. This was done in order to obtain representative concentrations of rising and falling water levels. As a consequence, only 2 - 3 measurements for each location and season were considered for calculations of ΔTA and ΔDIC.

#### 2.9.2. Wadden Sea – modelling the exchange rates

Grashorn (2015) performed the hydrodynamic computations of exchanged water masses (*wad_exc*) with FVCOM (Chen et al., 2003) by adding up the cumulative seaward transport during falling water level (tidal prisms) between the back-barrier islands that were located near the respective ECOHAM cells with adjacent Wadden Sea area. These values are given in Table 3 for each ECOHAM cell in the respective export areas. The definition of the first cell N1 and the last cell E4 is in accordance to the clockwise order in Fig. 1 (right side). The overall runoff of all N-, J- and E-positions was 8.1 $km^3\ d^{-1}$, 0.8 $km^3\ d^{-1}$ and 2.3 $km^3 d^{-1}$ respectively.

### *2.10. Model Setup*

The years 2001 to 2009 were simulated with 3 spin up years in 2000. Two different scenarios (A and B) were conducted. Scenario A is the reference scenario without implementation of any Wadden Sea processes. Wadden Sea export rates of TA and DIC were implemented in

https://doi.org/10.5194/bg-2020-24
Preprint. Discussion started: 29 January 2020


the second scenario (B) as described above. The respective Wadden Sea export rates are shown in Fig. 2.

### *2.11. Statistical analysis*

A statistical overview of the simulation results in comparison to the observations is given in Table 4. In the validation area (green box in Fig. 1) observations of 10 different stations were available, each with four to six measurements at different depths (51 measured points). Measured TA and DIC concentrations of each point were compared with modelled TA and DIC concentrations in the respective grid cells, respectively. The standard deviations (Stdv), the root mean square errors (RMSE), and correlation coefficients (r) were calculated for each simulation. One aim of this model development was to reduce the RMSE in order to bring the simulated TA concentrations closer to observations.

## 3. Results

### *3.1. Model validation - TA concentrations in summer 2008*

The results of scenarios A and B were compared with observations of TA in August 2008 (Salt et al., 2013). The observations revealed high TA concentrations in the German Bight (east of 7°E and south of 55°N) and around the Danish coast (around 56°N) as shown in Fig. 3a. The observed concentrations in these areas ranged between 2350 and 2387 µmol TA $kg^{-1}$. These findings were in accordance with observed TA concentrations in August / September 2001 (Thomas et al., 2009). TA concentrations in other parts of the observed domain ranged between 2270 µmol TA $kg^{-1}$ near the British coast (53°N – 56°N) and 2330 µmol TA $kg^{-1}$ near the Dutch coast and the Channel. In the validation box the overall average and the standard deviation of all observed TA concentrations (Stdv) was 2334 and 33 µmol TA $kg^{-1}$, respectively.

In scenario A the simulated surface TA concentrations showed a more homogeneous pattern than observations with maximum values of 2396 µmol TA $kg^{-1}$ at the western part of the Dutch coast and even higher (2450 µmol TA $kg^{-1}$) in the river mouth of the Wash estuary at the British coast. Minimum values of 2235 and 2274 µmol TA $kg^{-1}$ were simulated at the mouths of the rivers Elbe and Firth of Forth. The modelled TA concentration ranged from 2332 to 2351 µmol TA $kg^{-1}$ in the German Bight and in the Jade Bay. Strongest underestimations in relation to observations are located in a band close to the coast

https://doi.org/10.5194/bg-2020-24
Preprint. Discussion started: 29 January 2020


289 stretching from the East Frisian Islands to 57° N at the Danish coast (Fig. 5a). The deviation of
290 simulation results of scenario A from observations in the validation box was represented by
291 a RMSE of 28 µmol TA $kg^{-1}$. The standard variation was 7 µmol TA $kg^{-1}$ and the correlation
292 amounted to r=0.77 (Table 4).

293 The scenario B was based on a Wadden Sea export of TA and DIC as described above. The
294 major difference in TA concentrations of this scenario compared to A occurred east of 6.5°E.
295 There surface TA concentrations peaked in the Jade Bay (2769 µmol TA $kg^{-1}$) and were
296 elevated off the North Frisian and Danish coasts from 54.2° to 56° N (> 2400 µmol TA $kg^{-1}$ ).
297 Strongest overestimations in relation to observations appear off the Danish coast between
298 56 and 57° N (Fig. 5b). In the German Bight the observations were slightly overestimated,
299 while at the East Frisan Islands the model overestimates TA. When approaching the
300 Netherland's Frisian Islands the simulation underestimates TA compared to observations.
301 Near the river mouth of River Rhine stronger overestimations can be seen. Compared to
302 scenario A it was possible to bring the simulation closer to the observations (RMSE=18 µmol
303 TA $kg^{-1}$). Also the standard deviation (Stdv = 22 µmol TA $kg^{-1}$) and the correlation (r = 0.86)
304 improved (Table 4).
305

306 ***3.2. Model validation - DIC concentrations in summer 2008***

307 Analogously to TA the simulations were compared with surface observations of DIC
308 concentrations in summer 2008 (Salt et al., 2013). They also revealed high values in the
309 German Bight (east of 7 °E and south of 55°N) and around the Danish coast (near 56°N)
310 which is shown in Fig. 4. The observed DIC concentrations in these areas ranged between
311 2110 and 2173 µmol DIC $kg^{-1}$. Observed DIC concentrations in other parts of the model
312 domain ranged between 2030 and 2070 µmol DIC $kg^{-1}$ in the north western part and 2080 -
313 2117 µmol DIC $kg^{-1}$ at the Dutch coast. In the validation box the overall average and the
314 standard deviation of all observed DIC concentrations were 2108 and 25.09 µmol DIC $kg^{-1}$,
315 respectively.

316 The DIC concentrations in scenario A ranged between 1935 and 1977 µmol DIC $kg^{-1}$ at the
317 North Frisian- and Danish coasts (54.5°N - 55.5°N) and 1965 µmol DIC $kg^{-1}$ in the Jade Bay.
318 Maxima of up to 2164 µmol DIC $kg^{-1}$ were modelled at the western part of the Dutch coast
319 north of the mouth of River Rhine (Fig. 4). The DIC concentrations in the German Bight

https://doi.org/10.5194/bg-2020-24
Preprint. Discussion started: 29 January 2020


showed a heterogeneous pattern in the model, and sometimes values decreased from west to east, which is in contradiction to the observations (Fig. 4a). This may be the reason for the negative correlation coefficient r= -0.64 between model and observations (Table 5). The significant deviation from observation of results from scenario A is also indicated by the RMSE of 43 µmol DIC $kg^{-1}$, and a standard deviation of 14 µmol DIC $kg^{-1}$.

In scenario B the surface DIC concentrations at the Wadden Sea coasts increased: The North Frisian coast shows concentrations of up to 2200 µmol DIC$kg^{-1}$ while the German Bight has values of 2100 – 2160 µmol DIC $kg^{-1}$, and the Jade Bay concentrations were higher than 2250 µmol DIC $kg^{-1}$. The other areas are comparable to scenario A. In scenario B the RMSE in the validation box decreased to 26 µmol DIC $kg^{-1}$ in comparison to scenario A. The standard deviation decreased to 9.1 µmol DIC $kg^{-1}$, and the correlation improved and was r=0.55 (Table 5).

The comparison between observations and simulation results of scenario A (Fig. 5a) clearly show model underestimations in the south-eastern area, strongest in the inner German Bight towards the North Frisian coast (> 120 µmol DIC $kg^{-1}$). Scenario B still produces too low values in the south-eastern area (Fig. 5b), but the agreement between observation and model results is reasonable. Only off the Danish coast near 6.5°E, 56° N the model understimates DIC by 93 µmol DIC $kg^{-1}$.

### *3.3. Hydrodynamic conditions and flushing times*

The calculations of Wadden Sea TA export in Thomas et al. (2009) were based on several assumptions concerning riverine input of bulk TA and nitrate, atmospheric deposition of NOx, water column inventories of nitrate and the exchange between the Southern Bight and the adjacent North Sea (Lenhart et al., 1995). The latter was computed by considering that the water in the Southern Bight is flushed with water of the adjacent open North Sea at time scales of six weeks. For the study at hand, flushing times in the validation area in summer and winter are presented for the years 2001 to 2009 in Fig. 6. Additionally, monthly mean flow patterns of the model area are presented for June, July and August for the years 2003 and 2008, respectively (Fig. 7). They were chosen to highlight the pattern in summer 2003 with one of the highest flushing times, and that in 2008 corresponding to one of the lowest flushing times.

https://doi.org/10.5194/bg-2020-24
Preprint. Discussion started: 29 January 2020


The flushing times were calculated by dividing the total volume of the respective areas 1 – 3 by the total inflow into the areas $m^3$ ($m^3$ $s^{-1}$)$^{-1}$. Flushing times (rounded to integer values) were consistently higher in summer than in winter. Summer values in the whole validation area ranged from 54 days in 2008 to 81 days in 2003 and 2006, whereas the winter values in the same area ranged from 32 days in 2008 to 51 days in 2003 and 2009. The flushing times in the western and eastern part of the validation area were smaller due to the smaller box sizes. Due to the position, flushing times in the western part were consistently shorter than in the eastern part. These differences ranged from 5 days in winter 2002 to 14 days in summer 2006 and 2008. The interannual variabilities of all areas were higher in summer than in winter.

The North Sea is mainly characterised by an anti-clockwise circulation pattern (Otto et al., 1990; Pätsch et al., 2017). This can be observed for the summer months in 2008 (Fig. 7). More disturbed circulation patterns in the south-eastern part of the model domain occurred in June 2003: In the German Bight and in the adjacent western area two gyres with reversed rotating direction are dominant. In August 2003 the complete eastern part shows a clockwise rotation which is due to a meteorological blocking situation.

### 3.4. Seasonal and interannual variability of TA concentrations

The years 2001 to 2009 were simulated for the scenarios A and B. For both scenarios monthly mean surface concentrations of TA were calculated in the validation area and are shown in Fig. 8a and 8b. The highest TA-concentration in scenario A was 2329 µmol TA $kg^{-1}$ and occurred in July 2003. The lowest TA concentrations in each year were about 2313 to 2318 µmol TA $kg^{-1}$ and occurred in February and March. Scenario B showed generally higher values: Summer concentrations were in the range of 2348 to 2362 µmol TA $kg^{-1}$ and the values peaked in 2003. The lowest values occurred in the years 2004 – 2008. Also winter values were higher in scenario B than in scenario A: They range from 2322 to 2335 µmol TA $kg^{-1}$.

### 3.5. Seasonal and interannual variability of DIC concentrations

Along the lines of TA, monthly mean surface DIC concentrations in the validation area are shown in Fig. 8c and 8d. In scenario A the concentrations increased from October to

https://doi.org/10.5194/bg-2020-24
Preprint. Discussion started: 29 January 2020


February and decreased from March to August (Fig. 8c). In scenario B the time interval with increasing concentrations was extended into March. Maximum values of 2152 to 2172 µmol DIC $kg^{-1}$ in scenario A occur in February and March of each model year, and minimum values of 2060 to 2080 µmol DIC $kg^{-1}$ in August. Scenario B shows generally higher values: Highest values in February and March are 2161 to 2191 µmol DIC $kg^{-1}$. Lowest values in August range from 2095 to 2112 µmol DIC $kg^{-1}$. The amplitude of the annual cycle is smaller in scenario B, because the Wadden Sea export shows highest values in summer (Fig. 2).

## 4. Discussion

The aim of this study is to mechanistically test the estimates of Thomas et al. (2009) on the contributions of shallow intertidal and subtidal areas to the alkalinity budget of the SE North Sea. That estimate (by closure of mass fluxes) was about 73 Gmol TA $yr^{-1}$ originating from the Wadden Sea fringing the southern and eastern coast. These calculations were based on observations from the CANOBA dataset in 2001 and 2002. The observed high TA concentrations in the south eastern North Sea also were encountered in August 2008 (Salt et al., 2013) and these measurements were used for model validation in this study. Our simulations result in 39 Gmol TA $yr^{-1}$ as export from the Wadden Sea into the North Sea. A second aim is to differentiate between and quantify the individual sources. Former modelling studies of the carbonate system of the North Sea (Artioli et al., 2012, Lorkowski et al., 2012) did not consider the Wadden Sea as a source of TA and DIC. They showed good to reasonable agreement to observations from the CANOBA dataset in large parts of the North Sea in 2001 / 2002 (Thomas et al., 2009). Subsequent simulations that included TA export from aerobic and anaerobic processes in the sediment improved the agreement between data and models (Pätsch et al., 2018). When focusing on the German Bight, however, the observed high TA concentrations in summer measurements east of 7°E could not be simulated satisfactorily. The present study confirms the Wadden Sea as an important TA source for the German Bight and quantifies the annual Wadden Sea TA export rate to 39 Gmol TA $yr^{-1}$. Additionally, the contributions by most important rivers have been more precisely quantified and narrow down uncertainties in the budgets of TA and DIC in the

https://doi.org/10.5194/bg-2020-24
Preprint. Discussion started: 29 January 2020


German Bight. All steps that were required to calculate the budget including uncertainties are discussed in the following.

### *4.1. Uncertainties of Wadden Sea – German Bight exchange rates of TA and DIC*

The Wadden Sea is an area of effective benthic decomposition of organic material (Böttcher et al., 2004; Billerbeck et al., 2006; Al-Rai et al., 2009; van Beusekom et al., 2012) originating both from land and from the North Sea (Thomas et al., 2009). Anaerobic decomposition of the organic matter generates TA and increases the $CO_2$ buffer capacity of seawater. The Wadden Sea export rates of TA and DIC modelled in the present study are based on concentration measurements during tidal cycles in the years 2002 and 2009 to 2011 (Table 1), and on calculated tidal prisms of two day-periods that are considered to be representative of annual mean values. This approach introduces uncertainties with respect to the true amplitudes of concentrations differences in the tidal cycle and in seasonality due to the fact that differences in concentrations during falling and rising water levels were linearly interpolated. These interpolated values are based on four to five measurements in the three export areas and were conducted in different years. Consequently, the approach does not reproduce the exact TA and DIC concentrations in the years 2001 to 2009, because only meteorological forcing, river loads and nitrogen deposition were specified for these particular years. The simulation of scenario B thus only approximates Wadden Sea export rates. Nevertheless, the implementation of Wadden Sea export rates resulted in improved reproduction of observed high TA concentrations in the German Bight in summer (Fig. 3).

Primary processes that contribute to the TA generation in the Wadden Sea are denitrification, sulphate reduction, or processes that are coupled to sulphate reduction and other processes (Thomas et al., 2009). In our model, the implemented benthic denitrification does not generate TA (Seitzinger & Giblin, 1996), because modelled benthic denitrification does not consume nitrate (Pätsch & Kühn, 2008). Benthic denitrification is coupled to nitrification in the upper layer of the sediment (Raaphorst et al., 1990), giving reason for neglecting TA generation by this process in the model. The modelled production of $N_2$ by benthic denitrification falls in the range of 20 – 25 Gmol N $yr^{-1}$ in the validation area, which would result in a TA production of about 19 – 23 Gmol TA $yr^{-1}$ (Brenner et al., 2016). In the

https://doi.org/10.5194/bg-2020-24
Preprint. Discussion started: 29 January 2020


model nitrate uptake by phytoplankton is in the range of 40 Gmol TA $yr^{-1}$, which partly compensates the missing TA generation by benthic denitrification. Different from this, the TA budget of Thomas et al. (2009) included the entire benthic denitrification as a TA generating process.

Atmospheric nitrogen deposition is taken into account in the simulations. Oxidised N-species ($NO_x$) dominate reduced species ($NH_y$) slightly in the validation area during 6 out of 9 simulation years. This implies that the deposition of dissolved inorganic nitrogen decreases TA in 6 of 9 years. Thomas et al. (2009) also assumed a dominance of oxidised species and consequently defined a negative contribution to the TA budget.

Dissolution of biogenic carbonates may be an efficient additional source of TA, since most of the tidal flat surface sediments contain carbonate shell debris (Hild, 1997). On the other hand, oxidation of biogenic methane formed in deep and shallow tidal flat sediments (not modelled) (Höpner & Michaelis, 1994; Neira & Rackemann, 1996; Böttcher et al., 2007) is a source of DIC that counteracts carbonate dissolution.

The net effect of evaporation and precipitation in the Wadden Sea also has to be considered in budgeting TA. Although these processes are balanced in the North Sea (Schott, 1966), enhanced evaporation can occur in the Wadden Sea due to increased heating during low tide around noon. Onken & Riethmüller (2010) estimated an annual negative freshwater budget in the Hörnum Basin based on long-term hydrographic time series from observations in a tidal channel. From this data a mean salinity difference between flood and ebb currents of approximately -0.02 is calculated. This would result in an increasing TA concentration by 1 µmol TA $kg^{-1}$, which is the range of the inaccuracy of measurements. Furthermore, the enhanced evaporation estimated from subtle salinity changes interferes with potential input of submarine groundwater into the Wadden Sea, as has been identified by Moore et al. (2011) and Winde et al. (2014). The magnitude of this input is difficult to estimate at present, for example from salinity differences between flood and ebb tides, because the composition of SGD passing the sediment-water interfacial mixing zone has to be known. Although first characteristics have been reported (Moore et al., 2011; Winde et al., 2014), the quantitative effect of additional DIC, TA, and nutrient input via both fresh and recirculated SGD into the Wadden Sea remains unclear.

https://doi.org/10.5194/bg-2020-24
Preprint. Discussion started: 29 January 2020


An input of potential significance are small inlets that provide fresh water as well as DIC and TA (Table 6). The current data base for seasonal dynamics of this source, however, is patchy and this source cannot yet be considered quantitatively in budgeting approaches.

### *4.2. The impact of exported TA and DIC on the North Sea and influences on export magnitude*

Observed high TA and DIC concentrations in the SE North Sea are mainly caused by TA and DIC export from the Wadden Sea (Fig.3-5). TA concentrations could be better reproduced than DIC concentrations in the model experiments, which was mainly due to the higher sensitivity of DIC to modelled biology. Nevertheless, from a present point of view the Wadden Sea is the main driver of TA concentrations in the German Bight. Future forecast studies of the evolution of the carbonate system in the German Bight will have to specifically focus on the Wadden Sea and on processes occurring there. In this context the Wadden Sea evolution during future sea level rise is the most important factor. The balance between sediment supply from the North Sea and sea level rise is a general precondition for the persistence of the Wadden Sea (Flemming and Davis, 1994; Van Koningsveld et al., 2008). An accelerating sea level rise could lead to a deficient sediment supply from the North Sea and shift the balance at first in the largest tidal basins and at last in the smallest basins. (CPSL, 2001; Van Goor et al., 2003). The share of intertidal flats as potential sedimentation areas is larger in smaller tidal basins (van Beusekom et al., 2012), whereas larger basins have a larger share of subtidal areas. Thus, assuming an accelerating sea level rise, large tidal basins will turn into lagoons, while tidal flats may still exist in smaller tidal basins. This effect could decrease the overall Wadden Sea export rates of TA, because sediments would no longer be exposed to the atmosphere and the products of sulphate reduction would reoxidise in the water column. Moreover, benthic-pelagic exchange in the former intertidal flats would only be diffusive and no longer advective due to hydraulic gradients during ebb tides, when parts of the sediment become unsaturated with water. Caused by changes in hydrography and sea level the sedimentological composition may also change. If sediments become more sandy, aerobic degradation of organic matter is likely to become more dominant (de Beer et al., 2004). Regionally, the North Frisian Wadden Sea will be more affected by rising sea level

https://doi.org/10.5194/bg-2020-24
Preprint. Discussion started: 29 January 2020


because there the tidal basins are larger than the tidal basins in the East Frisian Wadden Sea and even larger than the inner Jade Bay.

The Wadden Sea export of TA and DIC is driven by the turnover of organic material. Decreasing anthropogenic eutrophication can lead to decreasing phytoplankton biomass and production (Cadée & Hegeman, 2002; van Beusekom et al., 2009). Thus, the natural variability of the North Sea primary production becomes more important in determining the organic matter turnover in the Wadden Sea (McQuatters-Gollop et al., 2007; McQuatters-Gollop & Vermaat, 2011). Moreover, despite the assumption of decreasing overall TA export rates from the Wadden Sea the impact of the North Frisian Wadden Sea on the carbonate system of the German Bight could potentially change due to a change of tidal prisms and thus a change in imported organic matter. If less organic matter is remineralised in the North Frisian Wadden Sea, less TA and DIC will be exported to the North Sea.

In the context of climate change, processes that have impact on the freshwater budget of tidal mud flats will gain in importance. Future climate change will have an impact in coastal hydrology due to changes in ground water formation rates (Faneca Sànchez et al., 2012; Sulzbacher et al., 2012), that may change both surface and subterranean run-off into the North Sea. An increasing discharge of small rivers and groundwater into the Wadden Sea is likely to increase DIC, TA, and possibly nutrient loads and may enhance the production of organic matter. Evaporation could also increase due to increased warming and become a more important process than today (Onken & Riethmüller, 2010).

Concluding, in the course of climate change the North Frisian Wadden Sea will be affected first by sea level rise, which will result in decreased TA and DIC export rates due to less turnover of organic matter there. This could lead to a decreased buffering capacity in the German Bight for atmospheric $CO_2$. Overall, less organic matter will be remineralised in the Wadden Sea.

### *4.3. TA budgets and variability of TA mass in the German Bight*

Modelled TA and DIC concentrations in the German Bight have a high interannual and seasonal variability (Fig. 8). Overall, the TA variability is more sensitive to Wadden Sea export rates than DIC variability, because the latter is dominated by biological processes. However,

https://doi.org/10.5194/bg-2020-24
Preprint. Discussion started: 29 January 2020


the implementation of Wadden Sea DIC export rates enabled a better reproduction of observed DIC concentrations in the near-coastal North Sea.

It is a logical step to attribute the TA variability to variabilities of the different sources. In order to calculate a realistic budget, scenario B was considered. Annual and seasonal budgets of TA sources and sinks in this scenario are shown in Table 2. Note that $Riv_{eff}$ is not taken into account for the budget calculations.

River input ranged from 78 to 152 Gmol TA $yr^{-1}$ and had the highest variability of all TA sources in the validation area. This is mostly due to the high variability of annual freshwater discharge, which is indicated by low (negative) values of $Riv_{eff}$. The latter values show that the riverine TA loads together with the freshwater flux induce a small dilution of TA in the validation area for each year. Comparing the absolute values of all sources and sinks of the mean year (only non-leap years were used) results in a relative ranking of the processes. 63 % of all TA mass changes in the validation area were due to net transport, 25 % were due to Wadden Sea export rates, 9 % were due to internal processes, and 3 % were due to river input $Riv_{eff}$ of TA (see chapter 2.6.2). Certainly, this ranking depends mainly on the characteristics of the Elbe estuary. Due to the high concentration of TA in rivers Rhine and Meuse (Netherlands) they had an effective river input of +24 Gmol TA $yr^{-1}$ in 2008, which constitutes a much greater impact on TA concentration changes than the Elbe river. In a sensitivity test, we switched off the TA loads of rivers Rhine and Meuse for the year 2008 and found that the net flow of -71 Gmol TA $yr^{-1}$ decreased to -80 Gmol TA $yr^{-1}$, which indicates that water entering the validation box from the western boundary is less TA-rich in the test case than in the reference run.

At seasonal time scales (Table 2 lower part) the net transport dominated the variations from October to March, while internal processes play a more important role from April to June (47 %). The impact of effective river input was smaller than 10% in every quarter. The Wadden Sea TA export rates had an impact of 59 % on TA mass changes in the validation area from July to September.

Summing up the sources and sinks, Wadden Sea exchange rates, internal processes and effective river loads resulted in highest sums in 2002 and 2003 (51 and 52 Gmol TA $yr^{-1}$) and lowest in 2009 (44 Gmol TA $yr^{-1}$). In agreement with this, the highest TA concentrations were

https://doi.org/10.5194/bg-2020-24
Preprint. Discussion started: 29 January 2020


simulated in summer 2003 (Fig. 8). The high interannual variability of summer concentrations was driven essentially by hydrodynamic differences between the years. Flushing times and their interannual variability were higher in summer than in winter (Fig. 6) of every year. High flushing times or less strong circulation do have an accumulating effect on exported TA in the validation area. To understand the reasons of the different flushing times monthly stream patterns were analysed (Fig. 7). Distinct anticlockwise stream patterns defined the hydrodynamic conditions in every winter. Summer stream patterns were in most years weaker, especially in the German Bight (compare Fig. 7 June 2003). In August 2003 the eastern part of the German Bight shows a clockwise rotation, which transports TA-enriched water from July back to the Wadden-Sea area for further enrichment. This could explain the highest concentrations in summer 2003.

One aim of this study was to recalculate the Wadden Sea TA export rates calculated by Thomas et al. (2009). They estimated that 73 Gmol TA $yr^{-1}$ were produced in the Wadden Sea. Their calculations were based on measurements in 2001 and 2002. The presented model was validated with data measured in August 2008 (Salt et al., 2013) at the same positions. High TA concentrations in the German Bight were observed in summer 2001 and in summer 2008. Due to the scarcity of data, the West Frisian Wadden Sea was not considered in the simulations, but the amount of exported TA from that area can safely be assumed to be in the same range as from the East Frisian Wadden Sea (10 to 14 Gmol TA $yr^{-1}$). With additional export from the West Frisian Wadden Sea, the maximum overall Wadden Sea export may be as high as 53 Gmol TA $yr^{-1}$. Thus, the TA export from the Wadden Sea calculated in this study is 20 to 34 TA Gmol $yr^{-1}$ lower than that assumed in the study of Thomas et al. (2009). This is mainly due to the flushing time that was assumed by Thomas et al. (2009). They considered the water masses to be flushed within six weeks (Lenhart et al., 1995). Flushing times calculated in the present study were significantly longer and more variable in summer. Since the Wadden Sea export calculated by Thomas et al. (2009) was defined as a closing term of the TA budget, underestimated summerly flushing times led to an overestimation of the exchange with the adjacent North Sea.

Another problematic aspect in the TA export estimate by Thomas et al. (2009) is the fact that their TA budget merges the sources of anaerobic TA generation from sediment and from the Wadden Sea into a single source “anaerobic processes in the Wadden Sea”. Burt et al. (2014)

https://doi.org/10.5194/bg-2020-24
Preprint. Discussion started: 29 January 2020


591 found a sediment TA generation of 12 mmol TA $m^{-2}$ $d^{-1}$ at one station in the German Bight
592 based on Ra-measurements. This fits into the range of microbial gross sulfate reduction rates
593 measured by Al-Raei et al. (2009) in the tidal areas of Spiekeroog island, and by Brenner et
594 al. (2016) at the Dutch coast. Within the latter paper, the different sources of TA from the
595 sediment were quantified. The largest term was benthic calcite dissolution, which would be
596 cancelled out in terms of TA generation assuming a steady-state compensation by biogenic
597 calcite production. Extrapolating the southern North Sea TA generation (without calcite
598 dissolution) from the data for one station of Brenner et al. (2016) results in an annual TA
599 production of 12.2 Gmol in the German Bight (Area = 28.415 $km^2$). This is surely an upper
600 limit of sediment TA generation, as the measurements were done in summer when seasonal
601 fluxes are maximal. This calculation reduces the annual Wadden Sea TA generation
602 estimated by Thomas et al. (2009) from 73 to 60.8 Gmol, which is still higher than our
603 present estimate. In spite of the unidentified additional TA-fluxes, both the estimate by
604 Thomas et al. (2009) and our present model-based quantification confirm the importance of
605 the Wadden-Sea export fluxes of TA on the North Sea carbonate system at present and in
606 the future.

607
608

609 **4.4 TA / DIC ratios during the course of the year**

610

611 The overall (bulk) export rates for the Wadden Sea were calculated for DIC and TA as well in
612 the present study. Although the detailed processes in all compartments were not simulated
613 explicitly, the ratio of exported TA and DIC reflects the dominant underlying biogeochemical
614 processes (Chen & Wang, 1999; Zeebe & Wolf-Gladrow, 2001; Thomas et al. 2009; Sippo et
615 al., 2016; Wurgaft et al., 2019). Aerobic degradation of organic material results in a
616 reduction of TA due to both increasing nitrate and DIC concentrations, and is indicated by a
617 TA / DIC ratio of -0.16. Denitrification is indicated by a TA / DIC ratio of 1 and anaerobic
618 processes related to sulphate reduction of organic material are indicated by a TA / DIC ratio
619 of 2. Aerobic and anaerobic oxidation of upward diffusing methane would further impact the
620 TA / DIC ratio in opposite directions, but were not considered in the present study.

https://doi.org/10.5194/bg-2020-24
Preprint. Discussion started: 29 January 2020


The ratios of the export rates TA / DIC for the different export areas are depicted in Fig. 9. The pelagic TA / DIC ratio in the North Frisian Wadden Sea (NF) ranged between 0 and 0.5 in spring and summer. Aerobic degradation of organic material and denitrification were the dominant processes here. The ratio became negative in autumn, which was due to a negative ΔTA value and thus a consumption of TA (compare Tab. 1). This may reflect resuspension of the surface sediment due to increasing wind-induced hydrodynamic circulation, so that previously formed sedimentary pyrite was re-oxidized (e.g., Kowalski et al., 2013). The DIC export rate also had its minimum in autumn (Tab. 1), which was likely caused by a decreasing supply of organic material during this season (e.g., Kowalski et al., 2009).

The TA / DIC ratios in the Jade Bay were around 1 between January and April, but ranged between 1.5 and 2 from June until September, when sulphate reduction associated with organic matter and/or methane oxidation and pyrite burial became the dominant processes. Later in the year, the ratio decreased to -0.5 in autumn, when aerobic degradation and re-oxidation of pyrite may have occurred, promoted by increasing wind forces and associated re-suspension and sulphide oxidation of anoxic sediment layers (Kowalski et al., 2013). The DIC export rate had its minimum in autumn, again due to limited supply of organic matter (Tab. 1).

The TA / DIC ratio of the East Frisian Wadden Sea was about 1 in February, when denitrification dominated. A slightly negative ratio was found at the beginning of April when aerobic degradation of organic matter dominated. Denitrification dominated until June. In August the ratio increased to 2, because anaerobic degradation processes became more important. Afterwards the ratios increased up to 3 in autumn, mainly due to relatively high ΔTA values (16 µmol $kg^{-1}$) compared to ΔDIC values (5 µmol $kg^{-1}$) (compare Tab. 1). This was caused by dominating processes related to organotrophic sulphate reduction. The maximum ratio of 3 may reflect a short-term effect of iron reduction that influenced the measurements of TA concentrations. Iron reduction leads to a high generation of TA on only short time scales, because reduced iron is rapidly re-oxidised to lower TA.

Based on these results, the North Frisian Wadden Sea export area showed a different pattern when compared to the East Frisian Wadden Sea and the Jade Bay areas. Aerobic degradation of organic matter played a key role in the North Frisian Wadden Sea during

https://doi.org/10.5194/bg-2020-24
Preprint. Discussion started: 29 January 2020


spring and summer. The DIC export rates indicate that most organic matter was degraded there, which may have been controlled by higher daily exchanged water masses in the North Frisian (8.1 $km^3\ d^{-1}$) than in the East Frisian Wadden Sea (2.3 $km^3\ d^{-1}$) and in the Jade Bay (0.8 $km^3\ d^{-1}$) (compare Tab. 3). On the other hand, TA export rates of the North Frisian and the East Frisian Wadden Sea were in the same range. Regional differences in organic matter dynamics in the Wadden Sea have already been discussed by van Beusekom et al. (2012). They suggested that the organic matter turnover in the Wadden Sea is overall driven by OM import from the North Sea, but that regionally different eutrophication effects modulate the general pattern. The reason for these differences is related to the shape and size of the individual tidal basins. Van Beusekom et al. (2012) proposed that wider tidal basins with a large distance between barrier islands and mainland generally have a lower eutrophication status than narrower ones. This may lead to a “dilution” effect of the imported organic matter in wider tidal basins. Therefore, aerobic degradation of organic matter dominated in the North Frisian Wadden Sea, where the distance between barrier islands and mainland is large. This leads to less eutrophication than in the East Frisian Wadden Sea, where anaerobic degradation of organic matter dominated in more restricted tidal basins.

https://doi.org/10.5194/bg-2020-24
Preprint. Discussion started: 29 January 2020


## 5. Conclusion

We presented a budget calculation of TA sources in the German Bight and related 25 % of the annual TA mass changes to Wadden Sea exports of TA. The impact of riverine bulk TA is less important in the German Bight than the contribution from the Wadden Sea due to the comparatively low TA concentrations in the Elbe estuary. Nevertheless, the rivers are sources of allochthonous nitrate, and denitrification of which in sediments is a major source for net TA generation.

The evolution of the carbonate system in the German Bight under future anthropogenic or climate change depends on the evolution of the Wadden Sea. The amount of TA and DIC that is exported from the Wadden Sea depends on the amount of organic matter that is imported from the North Sea and remineralised in the Wadden Sea. Decreasing riverine nutrient loads have led to decreasing phytoplankton biomass and production (Cadée & Hegeman, 2002; van Beusekom et al., 2009), a trend that is expected to continue. However, altered natural dynamics of nutrient cycling and productivity can override the decreasing riverine nutrient loads (van Beusekom et al., 2012), but these will not generate TA in the magnitude of denitrification of riverborne nitrate.

In the context of sea level rise, the North Frisian Wadden Sea will potentially be more affected by a loss of intertidal areas than the East Frisian Wadden Sea (van Beusekom et al., 2012). This effect is likely to reduce the turnover of organic material in this sector of the Wadden Sea, which will decrease TA production and decrease the overall input into the southern North Sea.

Thomas et al. (2009) estimated that the Wadden Sea facilitates approximately 7 – 10% of the annual $CO_2$ uptake of the North Sea. This is motivation for model studies on the future role of the Wadden Sea in the $CO_2$ balance of the North Sea under regional climate change. Future research will also have to address the composition and amount of submarine ground water discharge, as well as the magnitude and seasonal dynamics in discharge and composition of small water inlets at the coast which are currently ignored due to a lacking data base.

https://doi.org/10.5194/bg-2020-24
Preprint. Discussion started: 29 January 2020




**Acknowledgements**

Ina Lorkowski, Wilfried Kühn and Fabian Große are acknowledged for stimulating discussions. This work was financially supported by BMBF during the Joint Research Project BIOACID (TP 5.1, support code 03F0608L and TP 3.4.1, support code 03F0608F), with further support from Leibniz Institute for Baltic Research. We acknowledge the support by the Cluster of Excellence 'CliSAP' (EXC177), University of Hamburg, funded by the German Science Foundation (DFG) and the support by the German Academic Exchange service (DAAD, MOPGA-GRI, #57429828) with funds of the German Federal Ministry of Education and Research (BMBF).

https://doi.org/10.5194/bg-2020-24
Preprint. Discussion started: 29 January 2020




## Tables

**Table 1: Mean TA and DIC concentrations [µmol $kg^{-1}$] during rising and falling water levels and the respective differences (Δ-values) that were used as wad_sta in (1). Areas are the North Frisian (NF), the East Frisian (EF) Wadden Sea and the Jade Bay (JB).**

| Area | Date | TA (rising) | TA (falling) | ΔTA | DIC (rising) | DIC (falling) | ΔDIC |
|---|---|---|---|---|---|---|---|
| NF | 29.04.2009 | 2343 | 2355 | 12 | 2082* | 2106 | 24 |
| | 17.06.2009 | 2328 | 2332 | 4 | 2170 | 2190 | 20 |
| | 26.08.2009 | 2238 | 2252 | 14 | 2077 | 2105 | 28 |
| | 05.11.2009 | 2335 | 2333 | -2 | 2205 | 2209 | 4 |
| JB | 20.01.2010 | 2429 | 2443 | 14 | 2380 | 2392 | 12 |
| | 21.04.2010 | 2415 | 2448 | 33 | 2099 | 2132 | 33 |
| | 26.07.2010 | 2424 | 2485 | 61 | 2159 | 2187 | 28 |
| | 09.11.2010 | 2402 | 2399 | -3 | 2302 | 2310 | 8 |
| EF | 03.03.2010 | 2379 | 2393 | 14 | 2313 | 2328 | 15 |
| | 07.04.2010 | 2346 | 2342 | -4 | 2068 | 2082 | 14 |
| | 17./18.05.2011 | 2445 | 2451 | 6 | 2209 | 2221 | 12 |
| | 20.08.2002 | 2377 | 2414 | 37 | 2010 | 2030 | 20 |
| | 01.11.2010 | 2423 | 2439 | 16 | 2293 | 2298 | 5 |

*: This value was estimated.

https://doi.org/10.5194/bg-2020-24
Preprint. Discussion started: 29 January 2020




724 **Table 2: Annual TA budgets in the validation area of the years 2001 to 2009 and seasonal**
725 **budgets of the non-leave average years from January to March, April to June, July to**
726 **September and October to December [Gmol]. Net Flow is the amount of TA that passes the**
727 **validation area. Negative values indicate a net export from the validation area to the**
728 **adjacent North Sea. Δcontent indicates the difference of the TA contents of the last and**
729 **the first time steps of the simulated year or quarter.**

| | Wadden Sea | internal processes | river loads | $Riv_{eff}$ | net flow | Δcontent |
|---|---|---|---|---|---|---|
| | Gmol/yr | Gmol/yr | Gmol/yr | Gmol/yr | Gmol/yr | Gmol |
| 2001 | 39 | 13 | 87 | -5 | 38 | 177 |
| 2002 | 39 | 19 | 152 | -7 | -223 | -13 |
| 2003 | 39 | 16 | 91 | -3 | -98 | 48 |
| 2004 | 39 | 13 | 78 | -5 | -8 | 122 |
| 2005 | 39 | 12 | 89 | -5 | -98 | 42 |
| 2006 | 39 | 12 | 88 | -4 | -56 | 83 |
| 2007 | 39 | 12 | 110 | -5 | -132 | 29 |
| 2008 | 39 | 14 | 93 | -5 | -71 | 75 |
| 2009 | 39 | 10 | 83 | -5 | -151 | -19 |
| t = 3 mon | Gmol/t | Gmol/t | Gmol/t | Gmol/t | Gmol/t | Gmol |
| Jan - Mar | 8 | -1 | 38 | -1 | -57 | -12 |
| Apr - Jun | 10 | 14 | 23 | -2 | 4 | 51 |
| Jul - Sep | 17 | -2 | 15 | -2 | 8 | 38 |
| Oct - Dec | 4 | 2 | 24 | 0 | -58 | -28 |

730

731
732

733

https://doi.org/10.5194/bg-2020-24
Preprint. Discussion started: 29 January 2020




734
735

736 **Table 3: Daily Wadden Sea runoff to the North Sea at different export areas.**

| Position | wad_exc [$10^6$ $m^3$ $d^{-1}$] |
|---|---|
| N1 | 273 |
| N2 | 1225 |
| N3 | 1416 |
| N4 | 1128 |
| N5 | 4038 |
| N6 | 18 |
| J1 - J3 | 251 |
| E1 | 380 |
| E2 | 634 |
| E3 | 437 |
| E4 | 857 |

737

738

https://doi.org/10.5194/bg-2020-24
Preprint. Discussion started: 29 January 2020




739 **Table 4: Averages (µmol kg$^{-1}$), standard deviations (µmol kg$^{-1}$), RMSE (µmol kg$^{-1}$), and**
740 **correlation coefficients r for the observed TA concentrations and the corresponding**
741 **scenarios A and B within the validation area.**

| TA | Average | Stdv | RMSE | r |
|---|---|---|---|---|
| Obs | 2333.52 | 32.51 | | |
| A | 2327.64 | 6.84 | 27.97 | 0.77 |
| B | 2338.60 | 22.09 | 18.34 | 0.86 |

742

743
744

745 **Table 5: Averages (µmol kg$^{-1}$), standard deviations (µmol kg$^{-1}$), RMSE (µmol kg$^{-1}$), and**
746 **correlation coefficients r for the observed DIC concentrations and the corresponding**
747 **scenarios A and B within the validation area.**

748

| DIC | Average | Stdv | RMSE | r |
|---|---|---|---|---|
| Obs | 2107.05 | 24.23 | | |
| A | 2080.93 | 14.24 | 43.48 | -0.64 |
| B | 2091.15 | 9.25 | 25.87 | 0.55 |

749

750

751

752

753

https://doi.org/10.5194/bg-2020-24
Preprint. Discussion started: 29 January 2020




754 **Table 6: Examples for the carbonate system composition of small fresh water inlets**
755 **draining into the Jade Bay and the backbarrier tidal area of Spiekeroog Island, given in**
756 **(µmol $kg^{-1}$). Winter results (W) (October 31st, 2010) are taken from Winde et al. (2014);**
757 **summer sampling (S) took place on May 20th, 2011.**

| Site | Position | DIC(W) | TA(W) | DIC(S) | TA(S) |
|---|---|---|---|---|---|
| Neuharlingersiel | 53°41.944 N 7°42.170 E | 2319 | 1773 | 1915 | 1878 |
| Harlesiel | 53°42.376 N 7°48.538 E | 3651 | 3183 | 1939 | 1983 |
| Wanger/Horumersiel | 53°41.015 N 8°1.170 E | 5405 | 4880 | 6270 | 6602 |
| Hooksiel | 53°38.421 N 8°4.805 E | 2875 | 3105 | 3035 | 3302 |
| Maade | 53°33.534 N 8°7.082 E | 5047 | 4448 | 5960 | 6228 |
| Mariensiel | 53°30.895 N 8°2.873 E | 6455 | 5904 | 3665 | 3536 |
| Dangaster Siel | 53°26.737N 8°6.577 E | 1868 | 1246 | 1647 | 1498 |
| Wappelersiel | 53°23.414 N 8°12.437 E | 1373 | 630 | 1358 | 1152 |
| Schweiburger Siel | 53°24.725 N 8°16.968 E | 4397 | 3579 | 4656 | 4493 |
| Eckenwarder Siel | 53°31.249 N 8°16.527 E | 6542 | 6050 | 2119 | 4005 |

758

https://doi.org/10.5194/bg-2020-24
Preprint. Discussion started: 29 January 2020


## 6. Figure Caption

Figure 1: Model domains of ECOHAM (red) and FVCOM (blue), positions of rivers 1 – 16 (left, see Table 2) and the Wadden Sea export areas grid cells (right). The green edges identify the validation area, western and eastern part separated by the green dashed line.

Figure 2: Monthly Wadden Sea export of DIC and TA [Gmol $mon^{-1}$] at the North Frisian coast (NF), East Frisian coast (EF) and the Jade Bay in scenario B.

Figure 3: Surface TA-concentrations [µmol TA $kg^{-1}$] in August 2008 observed (a) and simulated with scenario A (b) and B (c).

Figure 4: Surface DIC-concentrations [µmol DIC $kg^{-1}$] in August 2008 observed (a) and simulated with scenario A (b) and B (c).

Figure 5: Differences between TA surface summer observations and results from scenario A (a) and B (b) and the differences between DIC surface observations and results from scenario A (c) and B (d), all in µmol $kg^{-1}$.

Figure 6: Flushing times in the validation area in summer (June to August) and winter (January to March). The whole validation area is represented in blue, green is the western part of the validation area (4.5°E to 7°E) and red is the eastern part (east of 7°E).

Figure 7: Monthly mean simulated streamlines for summer months 2003 and 2008.

Figure 8: Simulated monthly mean concentrations of TA (scenario A (a), scenario B (b)) [µmol TA $kg^{-1}$] and DIC (scenario A (c), scenario B (d)) [µmol DIC $kg^{-1}$] in the validation area for the years 2001-2009.

Fig. 9: Temporal interpolated TA/DIC ratio of the export rates in the North Frisian, East Frisian, and Jade Bay.

https://doi.org/10.5194/bg-2020-24
Preprint. Discussion started: 29 January 2020




## 7. References

Al-Rai, A.M., Bosselmann, K., Böttcher, M.E., Hespenheide, B., Tauber, F.: Seasonal dynamics of microbial sulfate reduction in temperate intertidal surface sediments: Controls by temperature and organic matter. Ocean Dynamics 59, 351-370, 2009.

Amann, T., Weiss, A., and Hartmann, J.: Inorganic Carbon Fluxes in the Inner Elbe Estuary, Germany, Estuaries and Coasts 38(1), 192-210, doi:10.1007/s12237-014-9785-6, 2015.

Artioli, Y., Blackford, J. C., Butenschön, M., Holt, J. T., Wakelin, S. L., Thomas, H., Borges, A. V., and Allen, J. I.: The carbonate system in the North Sea: Sensitivity and model validation, Journal of Marine Systems, 102-104, 1-13, doi:10.1016/j.jmarsys.2012.04.006, 2012.

Backhaus, J.O.: A three-dimensional model for the simulation of shelf sea dynamics, Ocean Dynamics, 38(4), 165–187, doi:10.1016/0278-4343(84)90044-X, 1985.

Backhaus, J.O., and Hainbucher, D.: A finite difference general circulation model for shelf seas and its application to low frequency variability on the North European Shelf, Elsevier Oceanography Series, 45, 221–244, doi:10.1016/S0422-9894(08)70450-1, 1987.

Berner, R. A., Scott, M. R., and Thomlinson, C.: Carbonate alkalinity in the pore waters of anoxic marine sediments. Limnology & Oceanography, 15, 544–549, doi:10.4319/lo.1970.15.4.0544, 1970.

Billerbeck, M., Werner, U., Polerecky, L., Walpersdorf, E., de Beer, D., Hüttel, M.: Surficial and deep pore water circulation governs spatial and temporal scales of nutrient recycling in intertidal sand flat sediment. Mar Ecol Prog Ser 326, 61-76, 2006.

Böttcher, M.E., Al-Raei, A.M., Hilker, Y., Heuer, V., Hinrichs, K.-U., Segl, M.: Methane and organic matter as sources for excess carbon dioxide in intertidal surface sands: Biogeochemical and stable isotope evidence. Geochimica et Cosmochim Acta 71, A111, 2007.

https://doi.org/10.5194/bg-2020-24
Preprint. Discussion started: 29 January 2020


815 Böttcher, M.E., Hespenheide, B., Brumsack, H.-J., Bosselmann, K.: Stable isotope
816 biogeochemistry of the sulfur cycle in modern marine sediments: I. Seasonal dynamics in a
817 temperate intertidal sandy surface sediment. Isotopes Environ. Health Stud. 40, 267-283,
818 2004.
819
820 Borges, A. V.: Present day carbon dioxide fluxes in the coastal ocean and possible feedbacks
821 under global change, In Oceans and the atmospheric carbon content (P.M. da Silva Duarte &
822 J.M. Santana Casiano Eds), Chapter 3, 47-77, doi:10.1007/978-90-481-9821-4, 2011.
823
824 Burt, W. J., Thomas, H., Pätsch, J., Omar, A. M., Schrum, C., Daewel, U., Brenner, H., and de
825 Baar, H. J. W.: Radium isotopes as a tracer of sediment-water column exchange in the North
826 Sea, Global Biogeochemical Cycles 28, pp 19, doi:10.1002/2014GB004825, 2014.
827
828 Burt, W. J., Thomas, H., Hagens, M., Pätsch, J., Clargo, N. M., Salt, L. A., Winde, V., and
829 Böttcher, M. E.: Carbon sources in the North Sea evaluated by means of radium and stable
830 carbon isotope tracers, Limnology and Oceanography, 61(2), 666-683,
831 doi:10.1002/lno.10243, 2016.
832
833 Brasse, J., Reimer, A., Seifert, R., and Michaelis, W.: The influence of intertidal mudflats on
834 the dissolved inorganic carbon and total alkalinity distribution in the German Bight,
835 southeastern North Sea, J. Sea Res. 42, 93-103, doi: 10.1016/S1385-1101(99)00020-9, 1999.
836
837 Brenner, H., Braeckman, U., Le Guitton, M., Meysman, F. J. R.: The impact of sedimentary
838 alkalinity release on the water column CO2 system in the North Sea, Biogeosciences, 13(3),
839 841-863, doi:10.5194/bg-13-841-2016, 2016.
840
841 Cadée, G. C., and Hegeman, J.: Phytoplankton in the Marsdiep at the end of the 20th century;
842 30 years monitoring biomass, primary production, and Phaeocystis blooms, J. Sea Res. 48,
843 97-110, doi:10.1016/S1385-1101(02)00161-2, 2002.
844
845 Cai, W.-J., Hu, X., Huang, W.-J., Jiang, L.-Q., Wang, Y., Peng, T.-H., and Zhang, X.: Surface
846 ocean alkalinity distribution in the western North Atlantic Ocean margins, Journal of

https://doi.org/10.5194/bg-2020-24
Preprint. Discussion started: 29 January 2020


847 Geophysical Research, 115, C08014, doi:10.1029/2009JC005482, 2010.
848
849 Carvalho, A. C. O., Marins, R. V., Dias, F. J. S., Rezende, C. E., Lefèvre, N., Cavalcante, M. S.,
850 and Eschrique, S. A.: Air-sea CO2 fluxes for the Brazilian northeast continental shelf in a
851 climatic transition region, Journal of Marine Systems, 173, 70-80,
852 doi:10.1016/j.jmarsys.2017.04.009, 2017.
853
854 Chambers, R. M., Hollibaugh, J. T., and Vink, S. M.: Sulfate reduction and sediment
855 metabolism in Tomales Bay, California, Biogeochemistry, 25, 1–18, doi:10.1007/BF00000509,
856 1994.
857
858 Chen, C.-T. A., Wang, S.-L.: Carbon, alkalinity and nutrient budgets on the East China Sea
859 continental shelf. Journal of Geophysical Research, 104, 20,675–20,686,
860 doi:10.1029/1999JC900055, 1999.
861
862 Chen, C., Liu, H., and Beardsley, R. C.: An Unstructured Grid, Finite-Volume, Three-
863 Dimensional, Primitive Equations Ocean Model: Application to Coastal Ocean and Estuaries, J
864 Atmos Oceanic Technol, 20 (1), 159-186,
865 doi:10.1175/1520-0426(2003)020<0159:AUGFVT>2.0.CO;2, 2003.
866
867 CPSL, 2001. Final Report of the Trilateral Working Group on Coastal Protection and Sea Level
868 Rise. Wadden Sea Ecosystem No. 13. Common Wadden Sea Secretariat, Wilhelmshaven,
869 Germany.
870
871 de Beer, D., Wenzhöfer, F., Ferdelman, T.G., Boehme, S., Huettel, M., van Beusekom, J.,
872 Boettcher, M., Musat, N., Dubilier, N.: Transport and mineralization rates in North Sea sandy
873 intertidal sediments (Sylt-Rømø Basin, Waddensea). Limnol. Oceanogr. 50, 113-127, 2004.
874
875 Dickson, A.G., Afghan, J.D., Anderson, G.C.: Reference materials for oceanic $CO_2$ analysis: a
876 method for the certification of total alkalinity. Marine Chemistry 80, 185-197, 2003.
877
878 Dollar, S. J., Smith, S. V., Vink, S. M., Obrebski, S., and Hollibaugh, J.T.: Annual cycle of

https://doi.org/10.5194/bg-2020-24
Preprint. Discussion started: 29 January 2020


879 benthic nutrient fluxes in Tomales Bay, California, and contribution of the benthos to total
880 ecosystem metabolism, Marine Ecology Progress Series, 79, 115–125,
881 doi:10.3354/meps079115, 1991.
882
883 Ehlers, J.: Geomorphologie und Hydrologie des Wattenmeeres. In: Lozan, J.L., Rachor, E., Von
884 Westernhagen, H., Lenz, W. (Eds.), Warnsignale aus dem Wattenmeer. Blackwell
885 Wissenschaftsverlag, Berlin, pp. 1–11. 1994.
886
887 Faneca Sànchez, M., Gunnink, J. L., van Baaren, E. S., Oude Essink, G. H. P., Siemon, B.,
888 Auken, E., Elderhorst, W., de Louw, P. G. B.: Modelling climate change effects on a Dutch
889 coastal groundwater system using airborne electromagnetic measurements. Hydrol. Earth
890 Syst. Sci. 16(12), 4499-4516, 2012.
891
892 Flemming, B. W., and Davis, R. A. J.: Holocene evolution, morphodynamics and
893 sedimentology of the Spiekeroog barrier island system (southern North Sea). Senckenb.
894 Marit. 25, 117-155, 1994.
895
896 Große, F., Kreus, M., Lenhart, H.-J., Pätsch, J., and Pohlmann,T.: A Novel Modeling Approach
897 to Quantify the Influence of Nitrogen Inputs on the Oxygen Dynamics of the North Sea,
898 Frontiers in Marine Science 4(383), pp 21, doi:10.3389/fmars.2017.00383, 2017.
899
900 Grashorn, S., Lettmann, K. A., Wolff, J.-O., Badewien, T. H., and Stanev, E. V.: East Frisian
901 Wadden Sea hydrodynamics and wave effects in an unstructured-grid model, Ocean
902 Dynamics 65(3), 419-434, doi:10.1007/s10236-014-0807-5, 2015.
903
904 HASEC: OSPAR Convention for the Protection of the Marine Environment of the North-East
905 Atlantic. Meeting of the Hazardous Substances and Eutrophication Committee (HASEC), Oslo
906 27 February – 2 March 2012.
907
908 Hild, A.: Geochemie der Sedimente und Schwebstoffe im Rückseitenwatt von Spiekeroog
909 und ihre Beeinflussung durch biologische Aktivität. Forschungszentrum Terramare Berichte

https://doi.org/10.5194/bg-2020-24
Preprint. Discussion started: 29 January 2020




910 5, 71 pp., 1997.

911 Höpner, T., Michaelis, H.: Sogenannte ‚Schwarze Flecken' – ein Eutrophierungssymptom des
912 Wattenmeeres. In: L. Lozán, E. Rachor, K. Reise, H. von Westernhagen und W. Lenz.
913 Warnsignale aus dem Wattenmeer. Berlin: Blackwell, 153-159, 1997.
914
915 Hoppema, J. M. J.; The distribution and seasonal variation of alkalinity in the southern bight
916 of the North Sea and in the western Wadden Sea, Netherlands Journal of Sea Research, 26
917 (1), 11-23, doi: 10.1016/0077-7579(90)90053-J, 1990.
918
919 Johannsen, A., Dähnke, K., and Emeis, K.-C.: Isotopic composition of nitrate in five German
920 rivers discharging into the North Sea, Organic Geochemistry, 39, 1678-1689
921 doi:10.1016/j.orggeochem.2008.03.004, 2008.
922
923 Johnson, K.M., Wills, K.D., Buttler, D.B., Johnson, W.K., Wong, C.S.: Coulometric total carbon
924 dioxide analysis for marine studies: maximizing the performance of an automated gas
925 extraction system and coulometric detector. Marine Chemistry 44, 167-187, 1993.
926
927 Kalnay, E., Kanamitsu, M., Kistler, R., Collins, W., Deaven, D., Gandin, L., Iredell, M., Saha S.,
928 White, G., Woollen, J., Zhu, Y., Chelliah, M., Ebisuzaki, W., Higgins, W., Janowiak, J., Mo, K.C.,
929 Ropelewski, C., Wang, J., Leetmaa, A., Reynolds, R., Jenne, R., and Joseph, D.: The
930 NCEP/NCAR 40-year reanalysis project, Bulletin of The American Meteorological Society,
931 77(3), 437–471, doi: 10.1175/1520-0477(1996)077<0437:TNYRP>2.0.CO;2, 1996.
932
933 Kempe, S. and Pegler, K.: Sinks and sources of CO2 in coastal seas: the North Sea, Tellus 43 B,
934 224-235, doi: 10.3402/tellusb.v43i2.15268, 1991.
935
936 Kerimoglu, O., Große, F., Kreus, M., Lenhart, H.-J., and van Beusekom, J. E. E.: A model-based
937 projection of historical state of a coastal ecosystem: Relevance of phytoplankton
938 stoichiometry, Science of The Total Environment 639, 1311-1323,
939 doi:10.1016/j.scitotenv.2018.05.215, 2018.
940

https://doi.org/10.5194/bg-2020-24
Preprint. Discussion started: 29 January 2020


941 Kohlmeier, C., and Ebenhöh, W.: Modelling the biogeochemistry of a tidal flat ecosystem
942 with EcoTiM, Ocean Dynamics, 59(2), 393-415, doi: 10.1007/s10236-009-0188-3, 2009.
943
944 Kowalski, N., Dellwig, O., Beck, M., Grunwald, M., Fischer, S., Piepho, M., Riedel, T., Freund,
945 H., Brumsack, H.-J., Böttcher, M. E. Trace metal dynamics in the water column and pore
946 waters in a temperate tidal system: response to the fate of algae-derived organic matter.
947 Ocean Dynamics 59, 333-350, 2009.
948
949 Kowalski, N., Dellwig, O., Beck, M., Gräwe, U., Pierau, N., Nägler, T., Badewien, T., Brumsack,
950 H.-J., van Beusekom, J.E. & Böttcher, M. E. Pelagic molybdenum concentration anomalies
951 and the impact of sediment resuspension on the molybdenum budget in two tidal systems of
952 the North Sea. Geochimica et Cosmochimica Acta 119, 198-211, 2013.
953
954 Kühn, W., Pätsch, J., Thomas, H., Borges, A. V., Schiettecatte, L.-S., Bozec, Y., and Prowe, A. E.
955 F.: Nitrogen and carbon cycling in the North Sea and exchange with the North Atlantic-A
956 model study, Part II: Carbon budget and fluxes, Continental Shelf Research, 30, 1701-1716,
957 doi:10.1016/j.csr.2010.07.001, 2010.
958
959 Laruelle, G. G., Lauerwald, R., Pfeil, B., and Regnier, P.: Regionalized global budget of the CO2
960 exchange at the air-water interface in continental shelf seas, Global Biogeochemical Cycles,
961 28 (11), 1199-1214, doi: 10.1002/2014gb004832, 2014.
962
963 Lenhart, H.-J., Radach, G., Backhaus, J. O., and Pohlmann, T.: Simulations of the North Sea
964 circulation, its variability, and its implementation as hydrodynamical forcing in ERSEM, Neth.
965 J. Sea Res., 33, 271–299, doi:10.1016/0077-7579(95)90050-0, 1995.
966
967 Lettmann, K. A., Wolff, J.-O., and Badewien, T.H.: Modeling the impact of wind and waves on
968 suspended particulate matter fluxes in the East Frisian Wadden Sea (southern North Sea),
969 Ocean Dynamics, 59(2), 239-262, doi: 10.1007/s10236-009-0194-5, 2009.
970
971 Lipinski, M.: Nährstoffelemente und Spurenmetalle in Wasserproben der Hunte und Jade.
972 Diploma thesis, C.v.O. University of Oldenburg, 82 pp., 1999.

https://doi.org/10.5194/bg-2020-24
Preprint. Discussion started: 29 January 2020


973
974 Lorkowski, I., Pätsch, J., Moll, A., and Kühn, W.: Interannual variability of carbon fluxes in the
975 North Sea from 1970 to 2006 – Competing effects of abiotic and biotic drivers on the gas-
976 exchange of CO2, Estuarine, Coastal and Shelf Science, 100, 38-57,
977 doi:10.1016/j.ecss.2011.11.037, 2012.
978
979 McQuatters-Gollop, A., Raitsos, D. E., Edwards, M., Pradhan, Y., Mee, L. D., Lavender, S. J.,
980 Attrill, and M. J.: A long-term chlorophyll data set reveals regime shift in North Sea
981 phytoplankton biomass unconnected to nutrient trends, Limnology & Oceanography, 52,
982 635-648, doi:10.4319/lo.2007.52.2.0635, 2007.
983
984 McQuatters-Gollop, A., and Vermaat, J. E.: Covariance among North Sea ecosystem state
985 indicators during the past 50 years e contrasts between coastal and open waters, Journal of
986 Sea Research, 65, 284-292, doi:10.1016/j.seares.2010.12.004, 2011.
987
988 Moore, W.S., Beck, M., Riedel, T., Rutgers van der Loeff, M., Dellwig, O., Shaw, T.J.,
989 Schnetger, B., and Brumsack, H.-J.: Radium-based pore water fluxes of silica, alkalinity,
990 manganese, DOC, and uranium: A decade of studies in the German Wadden Sea, Geochimica
991 et Cosmochimica Acta, 75, 6535 – 6555, doi:10.1016/j.gca.2011.08.037, 2011.
992
993 Neal, C.: Calcite saturation in eastern UK rivers, The Science of the Total Environment, 282-
994 283, 311-326, doi:10.1016/S0048-9697(01)00921-4, 2002.
995
996 Neira, C., Rackemann, M.: Black spots produced by buried macroalgae in intertidal sandy
997 sediments of the Wadden Sea: effects on the meiobenthos. J. Sea Res., 36, 153 - 170, 1996.
998
999 Onken, R., and Riethmüller, R.: Determination of the freshwater budget of tidal flats from
1000 measurements near a tidal inlet, Continental Shelf Research, 30, 924-933,
1001 doi:10.1016/j.csr.2010.02.004, 2010.
1002
1003 Otto, L., Zimmerman, J.T.F., Furnes, G.K., Mork, M., Saetre, R., and Becker, G.: Review of the
1004 physical oceanography of the North Sea, Netherlands Journal of Sea Research, 26 (2-4), 161–


238, doi:10.1016/0077-7579(90)90091-T, 1990.

Pätsch, J., and Kühn, W.: Nitrogen and carbon cycling in the North Sea and exchange with the North Atlantic – a model study Part I: Nitrogen budget and fluxes, Continental Shelf Research, 28, 767–787, doi: 10.1016/j.csr.2007.12.013, 2008.

Pätsch, J., and Lenhart, H.-J.: Daily Loads of Nutrients, Total Alkalinity, Dissolved Inorganic Carbon and Dissolved Organic Carbon of the European Continental Rivers for the Years 1977–2006, Berichte aus dem Zentrum für Meeres- und Klimaforschung (https://wiki.cen.uni-hamburg.de/ifm/ECOHAM/DATA_RIVER), 2008.

Pätsch, J., Serna, A., Dähnke, K., Schlarbaum, T., Johannsen, A., and Emeis, K.-C.: Nitrogen cycling in the German Bight (SE North Sea) - Clues from modelling stable nitrogen isotopes. Continental Shelf Research, 30, 203-213, doi:10.1016/j.csr.2009.11.003, 2010.

Pätsch, J., Kühn, W., and Six, K. D.: Interannual sedimentary effluxes of alkalinity in the southern North Sea: model results compared with summer observations, Biogeosciences 15(11), 3293-3309, doi: 10.5194/bg-15-3293-2018, 2018.

Pätsch, J., Burchard, H., Dieterich, C., Gräwe, U., Gröger, M., Mathis, M., Kapitza, H., Bersch,M., Moll, A., Pohlmann, T., Su, J., Ho-Hagemann, H.T.M., Schulz, A., Elizalde, A., and Eden, C.: An evaluation of the North Sea circulation in global and regional models relevant for ecosystem simulations, Ocean Modelling, 116, 70-95, doi:10.1016/j.ocemod.2017.06.005, 2017.

Pohlmann, T.: Predicting the thermocline in a circulation model of the North Sea – Part I: model description, calibration and verification, Continental Shelf Research, 16(2), 131–146, doi:10.1016/0278-4343(95)90885-S, 1996.

Provoost, P., van Heuven, S., Soetaert, K., Laane, R. W. P. M., and Middelburg, J. J.: Seasonal and long-term changes in pH in the Dutch coastal zone, Biogeoscience, 7, 3869-3878, doi:10.5194/bg-7-3869-2010, 2010.

https://doi.org/10.5194/bg-2020-24
Preprint. Discussion started: 29 January 2020


1038 Raaphorst, W., Kloosterhuis H. T., Cramer, A., and Bakker, K. J. M.: Nutrient early diagenesis
1039 in the sandy sediments of the Dogger Bank area, North Sea: pore water results, Neth. J. Sea.
1040 Res., 26(1), 25-52, doi: 10.1016/0077-7579(90)90054-K, 1990.
1041
1042 Radach, G. and Pätsch, J.: Variability of Continental Riverine Freshwater and Nutrient Inputs
1043 into the North Sea for the Years 1977-2000 and Its Consequences for the Assessment of
1044 Eutrophication, Estuaries and Coasts 30(1), 66-81, doi: 10.1007/BF02782968, 2007.
1045
1046 Reimer, S., Brasse, S., Doerffer, R., Dürselen, C. D., Kempe, S., Michaelis, W., and Seifert, R.:
1047 Carbon cycling in the German Bight: An estimate of transformation processes and transport,
1048 Deutsche Hydr. Zeitschr. 51**,** 313-329, doi: /10.1007/BF02764179, 1999.
1049
1050 Riedel, T., Lettmann, K., Beck, M., Brumsack, H.-J..: Tidal variations in groundwater storage
1051 and associated discharge from an intertidal coastal aquifer. Journal of Geophysical Research
1052 115, 1-10, 2010.
1053
1054 Rullkötter, J.: The back-barrier tidal flats in the southern North Sea—a multidisciplinary
1055 approach to reveal the main driving forces shaping the system, Ocean Dynamics, 59(2), 157-
1056 165, doi: 10.1007/s10236-009-0197-2, 2009.
1057
1058 Salt, L. A., Thomas, H., Prowe, A. E. F., Borges, A. V., Bozec, Y., and de Baar, H. J. W.:
1059 Variability of North Sea pH and CO2 in response to North Atlantic Oscillation forcing, Journal
1060 of Geophysical Research, Biogeosciences, 118, pp 9, doi:10.1002/2013JG002306, 2013.
1061
1062 Santos, I. R., Eyre, B. D., and Huettel, M.: The driving forces of porewater and groundwater
1063 flow in permeable coastal sediments: A review, Estuarine, Coastal and Shelf Science, 98, 1-
1064 15, doi:10.1016/j.ecss.2011.10.024, 2012.
1065
1066 Santos, I. R., Beck, M., Brumsack, H.-J., Maher, D.T., Dittmar, T., Waska, H., and Schnetger,
1067 B.: Porewater exchange as a driver of carbon dynamics across a terrestrial-marine transect:
1068 Insights from coupled 222Rn and pCO2 observations in the German Wadden Sea, Marine
1069 Chemistry, 171, 10-20, doi:10.1016/j.marchem.2015.02.005, 2015.

https://doi.org/10.5194/bg-2020-24
Preprint. Discussion started: 29 January 2020


1070
1071 Schott, F.: Der Oberflächensalzgehalt in der Nordsee, Deutsche Hydr. Zeitschr., Reije A Nr. 9,
1072 SUPPL. A9, pp 1-29, 1966.
1073
1074 Schwichtenberg, F.: Drivers of the carbonate system variability in the southern North Sea:
1075 River input, anaerobic alkalinity generation in the Wadden Sea and internal processes,
1076 (Doktorarbeit/PhS), Universität Hamburg, Hamburg, Germany, 161 pp, 2013.
1077
1078 Seibert, S.L., Greskowiak J., Prommer H., Böttcher ME, Waska H., Massmann G.: Modeling
1079 biogeochemical processes in a barrier island freshwater lens (Spiekeroog, Germany). J.
1080 Hydrol., in press, 2019.
1081
1082 Seitzinger, S., and Giblin, A.E.: Estimating denitrification in North Atlantic continental shelf
1083 sediments, Biogeochemistry, 35, 235–260, doi: 10.1007/BF02179829, 1996.
1084
1085 Shadwick, E. H., Thomas, H., Azetsu-Scott, K., Greenan, B. J. W., Head, E., and Horne, E.:
1086 Seasonal variability of dissolved inorganic carbon and surface water pCO2 in the Scotian
1087 Shelf region of the Northwestern Atlantic, Marine Chemistry, 124 (1–4), 23-37,
1088 doi:10.1016/j.marchem.2010.11.004, 2011.
1089
1090 Sippo, J.Z., Maher, D.T., Tait, D.R., Holloway, C., Santos, I.R.: Are mangroves drivers or
1091 buffers of coastal acidification? Insights from alkalinity and dissolved inorganic carbon export
1092 estimates across a latitudinal transect. Global Biogeochemical Cycles, 30, 753-766, 2016.
1093
1094 Smith, S. V., and Hollibaugh, J. T.: Coastal metabolism and the oceanic organic carbon
1095 balance, Reviews of Geophysics, 31, 75–89, doi:10.1029/92RG02584, 1993.
1096
1097 Streif, H.: Das ostfriesische Wattenmeer. Nordsee, Inseln, Watten und Marschen. Gebrüder
1098 Borntraeger, Berlin, 1990.
1099
1100 Sulzbacher, H., Wiederhold, H., Siemon, B., Grinat, M., Igel, J., Burschil, T., Günther, T.,
1101 Hinsby, K.: Numerical modelling of climate change impacts on freshwater lenses on the

https://doi.org/10.5194/bg-2020-24
Preprint. Discussion started: 29 January 2020


1102 North Sea Island of Borkum using hydrological and geophysical methods." Hydrol. Earth Syst.
1103 Sci. 16(10): 3621-3643, 2012.

1104
1105 Thomas, H., Bozec, Y., Elkalay, K., and de Baar, H. J. W.: Enhanced open ocean storage of CO2
1106 from shelf sea pumping, Science, 304, 1005-1008, doi:10.1126/science.1095491, 2004.
1107
1108 Thomas, H., Schiettecatte, L.-S., Suykens, K., Kone, Y. J. M., Shadwick, E. H., Prowe, A. E. F.,
1109 Bozec, Y., De Baar, H. J. W., and Borges, A. V.: Enhanced ocean carbon storage from
1110 anaerobic alkalinity generation in coastal sediments, Biogeosciences, 6, 267-274,
1111 doi:10.5194/bg-6-267-2009, 2009.
1112
1113 Van Beusekom, J. E. E., Loebl, M., and Martens, P.: Distant riverine nutrient supply and local
1114 temperature drive the long-term phytoplankton development in a temperate coastal basin,
1115 J. Sea Res. 61, 26-33, doi:10.1016/j.seares.2008.06.005, 2009.
1116
1117 Van Beusekom, J. E. E., Buschbaum, C., and Reise, K.: Wadden Sea tidal basins and the
1118 mediating role of the North Sea in ecological processes: scaling up of management? Ocean &
1119 Coastal Management, 68, 69-78, doi:10.1016/j.ocecoaman.2012.05.002, 2012.
1120
1121 Van Goor, M. A., Zitman, T. J.,Wang, Z. B., and Stive, M. J. F.: Impact of sea-level rise on the
1122 equilibrium state of tidal inlets, Mar. Geol. 202, 211-227, doi:10.1016/S0025-3227(03)00262-
1123 7, 2003.
1124
1125 Van Koningsveld, M., Mulder, J. P. M., Stive, M. J. F., Van der Valk, L., and Van der Weck,
1126 A.W.: Living with sea-level rise and climate change: a case study of the Netherlands, J. Coast.
1127 Res. 24, 367-379, doi:10.2112/07A-0010.1, 2008.
1128
1129 Wang, Z. A., Cai, W.-J.: Carbon dioxide degassing and inorganic carbon export from a marsh-
1130 dominated estuary (the Duplin River): A marsh CO2 pump, Limnology & Oceanography, 49,
1131 341–354, doi:10.4319/lo.2004.49.2.0341, 2004.
1132

https://doi.org/10.5194/bg-2020-24
Preprint. Discussion started: 29 January 2020


1133 Winde, V.: Zum Einfluss von benthischen und pelagischen Prozessen auf das Karbonatsystem
1134 des Wattenmeeres der Nordsee. Dr.rer.nat. thesis, EMA University of Greifswald, 2013.

1135
1136 Winde, V., Böttcher, M. E., Escher, P., Böning, P., Beck, M., Liebezeit, G., and Schneider, B.:
1137 Tidal and spatial variations of DI$^{13}$C and aquatic chemistry in a temperate tidal basin during
1138 winter time, Journal of Marine Systems, 129, 396-404, doi:10.1016/j.jmarsys.2013.08.005,
1139 2014.
1140
1141 Wolf-Gladrow, D. A., Zeebe, R. E., Klaas, C., Kortzinger, A., and Dickson, A. G.: Total alkalinity:
1142 The explicit conservative expression and its application to biogeochemical processes, Marine
1143 Chemistry, 106, 287–300, doi:10.1016/j.marchem.2007.01.006, 2007.
1144
1145 Wurgaft E., Findlay A.J., Vigderovich H., Herut B., Sivan O.: Sulfate reduction rates in the
1146 sediments of the Mediterranean continental shelf inferred from combined dissolved
1147 inorganic carbon and total alkalinity profiles. Marine Chemistry, 211,64-74, 2019.
1148
1149 Zeebe, R.E., Wolf-Gladrow, D. 2001. CO2 in seawater: Equilibrium, Kinetics, Isotopes. 1$^{st}$ edn.
1150 ELSEVIER.
1151
1152
1153
1154
1155
1156
1157
1158
1159
1160
1161

https://doi.org/10.5194/bg-2020-24
Preprint. Discussion started: 29 January 2020




## 8. Appendix

**Table A1: Annual riverine freshwater discharge [km³ yr⁻¹]. The numbering refers to Fig. 1.**

| | 2001 | 2002 | 2003 | 2004 | 2005 | 2006 | 2007 | 2008 | 2009 |
|---|---|---|---|---|---|---|---|---|---|
| 1) Elbe | 23.05 | 43.38 | 23.95 | 19.56 | 25.56 | 26.98 | 26.61 | 24.62 | 24.28 |
| 2) Ems | 3.47 | 4.48 | 3.15 | 3.52 | 2.99 | 2.54 | 4.32 | 3.32 | 2.58 |
| 3) Noordzeekanaal | 3.21 | 2.98 | 2.49 | 3.05 | 3.03 | 2.96 | 1.55 | 3.05 | 2.46 |
| 4) Ijsselmeer (east) | 9.55 | 9.94 | 6.27 | 7.97 | 7.35 | 7.30 | 9.10 | 8.23 | 6.59 |
| 5) Ijsselmeer (west) | 9.55 | 9.94 | 6.27 | 7.97 | 7.35 | 7.30 | 9.10 | 8.23 | 6.59 |
| 6) Nieuwe Waterweg | 50.37 | 51.33 | 34.72 | 42.91 | 41.61 | 44.21 | 49.59 | 49.76 | 44.69 |
| 7) Haringvliet | 33.10 | 35.18 | 17.92 | 10.77 | 12.36 | 16.02 | 24.00 | 15.70 | 11.06 |
| 8) Scheldt | 7.28 | 2.74 | 4.31 | 3.64 | 3.59 | 3.74 | 4.63 | 4.57 | 3.63 |
| 9) Weser | 11.43 | 18.97 | 11.80 | 10.52 | 10.37 | 9.72 | 16.21 | 12.59 | 9.58 |
| 10) Firth of Forth | 2.72 | 3.76 | 2.06 | 3.01 | 3.00 | 2.84 | 2.85 | 3.59 | 3.66 |
| 11) Tyne | 1.81 | 2.25 | 1.18 | 2.04 | 1.92 | 1.78 | 2.09 | 2.70 | 2.05 |
| 12) Tees | 1.33 | 1.78 | 0.94 | 1.59 | 1.27 | 1.45 | 1.49 | 1.99 | 1.55 |
| 13) Humber | 10.76 | 12.10 | 7.16 | 10.51 | 7.68 | 11.11 | 12.03 | 13.87 | 9.60 |
| 14) Wash | 5.46 | 4.39 | 3.08 | 3.91 | 1.96 | 2.72 | 5.24 | 4.77 | 3.21 |
| 15) Thames | 4.47 | 3.23 | 2.41 | 2.13 | 0.96 | 1.57 | 3.52 | 3.20 | 2.38 |
| 16) Eider | 0.67 | 0.97 | 0.47 | 0.70 | 0.68 | 0.67 | 0.63 | 0.58 | 0.57 |
| Sum | 178.2 | 207.4 | 128.1 | 133.7 | 131.6 | 142.9 | 172.9 | 160.7 | 134.4 |

https://doi.org/10.5194/bg-2020-24
Preprint. Discussion started: 29 January 2020




1170 **Table A2: River numbers in Fig. 1, their positions and source of data**

| Number in Fig. 1 | Name | River mouth position | | Data source |
|---|---|---|---|---|
| 1 | Elbe | 53°53'20"N | 08°55'00" E | Pätsch & Lenhart (2008); TA-, DIC- and nitrate-concentrations by Amann (2015) |
| 2 | Ems | 53°29'20"N | 06°55'00"E | Pätsch & Lenhart (2008) |
| 3 | Noordzeekanaal | 52°17'20"N | 04°15'00"E | Pätsch & Lenhart (2008); TA-, DIC- and nitrate-concentrations from waterbase.nl |
| 4 | Ijsselmeer (east) | 53°17'20"N | 05°15'00"E | As above |
| 5 | Ijsselmeer (west) | 53°05'20"N | 04°55'00"E | As above |
| 6 | Nieuwe Waterweg | 52°05'20"N | 03°55'00"E | As above |
| 7 | Haringvliet | 51°53'20"N | 03°55'00"E | As above |
| 8 | Scheldt | 51°29'20"N | 03°15'00"E | As above |
| 9 | Weser | 53°53'20"N | 08°15'00"E | Pätsch & Lenhart (2008) |
| 10 | Firth of Forth | 56°05'20"N | 02°45'00"W | HASEC (2012) |
| 11 | Tyne | 55°05'20"N | 01°25'00"W | HASEC (2012) |
| 12 | Tees | 54°41'20"N | 01°05'00"W | HASEC (2012) |
| 13 | Humber | 53°41'20"N | 00°25'00"W | HASEC (2012) |
| 14 | Wash | 52°53'20"N | 00°15'00"E | HASEC (2012): sum of 4 rivers: Nene, Ouse, Welland and Witham |
| 15 | Thames | 51°29'20"N | 00°55'00"E | HASEC (2012) |
| 16 | Eider | 54°05'20"N | 08°55'00"E | Johannsen et al, 2008 |

1171

https://doi.org/10.5194/bg-2020-24
Preprint. Discussion started: 29 January 2020




1172 **Table A3: Values of TA, DIC concentrations [µmol kg$^{-1}$] of rivers**

| River parameter | Jan | Feb | Mar | Apr | May | Jun | Jul | Aug | Sep | Oct | Nov | Dec | mean |
|---|---|---|---|---|---|---|---|---|---|---|---|---|---|
| Elbe TA | 2380 | 2272 | 2293 | 2083 | 2017 | 1967 | 1916 | 1768 | 1988 | 2156 | 2342 | 2488 | 2139 |
| Noordzeekanaal TA | 3762 | 3550 | 3524 | 3441 | 4748 | 3278 | 3419 | 3183 | 3027 | 3299 | 3210 | 3413 | 3488 |
| Nieuwe Waterweg TA | 2778 | 2708 | 2765 | 3006 | 2883 | 2658 | 2876 | 2695 | 2834 | 2761 | 2834 | 2927 | 2810 |
| Haringvliet TA | 2588 | 2635 | 2532 | 3666 | 2826 | 2829 | 2659 | 2660 | 2496 | 2816 | 2758 | 2585 | 2754 |
| Scheldt TA | 3781 | 3863 | 3708 | 3725 | 3758 | 3626 | 3722 | 3514 | 3367 | 3666 | 3825 | 3801 | 3696 |
| Ijsselmeer TA | 2829 | 3005 | 2472 | 2259 | 2611 | 1864 | 1672 | 1419 | 1445 | 2172 | 2286 | 2551 | 2215 |
| Elbe DIC | 2415 | 2319 | 2362 | 2179 | 2093 | 2025 | 1956 | 1853 | 2018 | 2200 | 2428 | 2512 | 2197 |
| Noordzeekanaal DIC | 3748 | 3579 | 3470 | 3334 | 3901 | 3252 | 3331 | 3136 | 2977 | 3214 | 3183 | 3405 | 3378 |
| Nieuwe Waterweg DIC | 2861 | 2794 | 2823 | 2991 | 2879 | 2657 | 2886 | 2706 | 2828 | 2773 | 2907 | 3036 | 2845 |
| Haringvliet DIC | 2673 | 2735 | 2600 | 3661 | 2850 | 2846 | 2687 | 2681 | 2512 | 2859 | 2803 | 2670 | 2798 |
| Scheldt DIC | 3798 | 3909 | 3829 | 3737 | 3704 | 3592 | 3705 | 3490 | 3316 | 3648 | 3733 | 3868 | 3694 |
| Ijsselmeer DIC | 2824 | 3008 | 2458 | 2234 | 2576 | 1826 | 1636 | 1369 | 1399 | 2134 | 2285 | 2565 | 2193 |
| Elbe $NO_3$ | 247 | 330 | 277 | 225 | 193 | 161 | 129 | 103 | 112 | 157 | 267 | 164 | 197 |
| Noordzeekanaal $NO_3$ | 150 | 168 | 190 | 118 | 79 | 71 | 64 | 73 | 78 | 92 | 107 | 137 | 111 |
| Nieuwe Waterweg $NO_3$ | 232 | 243 | 231 | 195 | 150 | 140 | 132 | 135 | 113 | 145 | 201 | 220 | 178 |
| Haringvliet $NO_3$ | 233 | 252 | 218 | 200 | 143 | 144 | 133 | 117 | 128 | 127 | 143 | 228 | 172 |
| Scheldt $NO_3$ | 320 | 341 | 347 | 345 | 243 | 221 | 219 | 215 | 189 | 202 | 190 | 274 | 259 |
| Ijsselmeer $NO_3$ | 136 | 159 | 190 | 192 | 135 | 46 | 20 | 14 | 7 | 18 | 20 | 79 | 85 |

https://doi.org/10.5194/bg-2020-24
Preprint. Discussion started: 29 January 2020


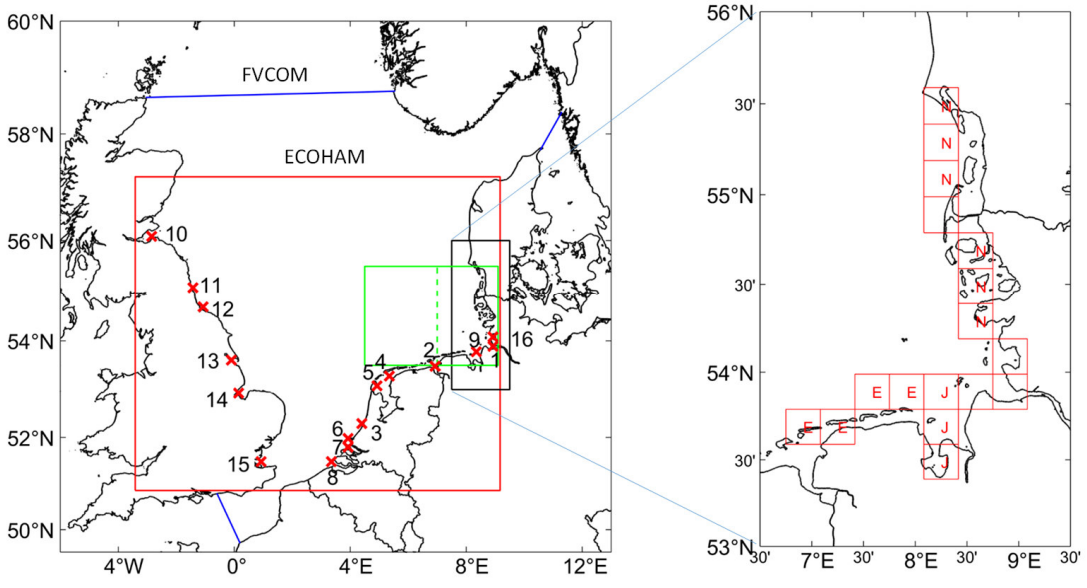


Fig. 1

https://doi.org/10.5194/bg-2020-24
Preprint. Discussion started: 29 January 2020


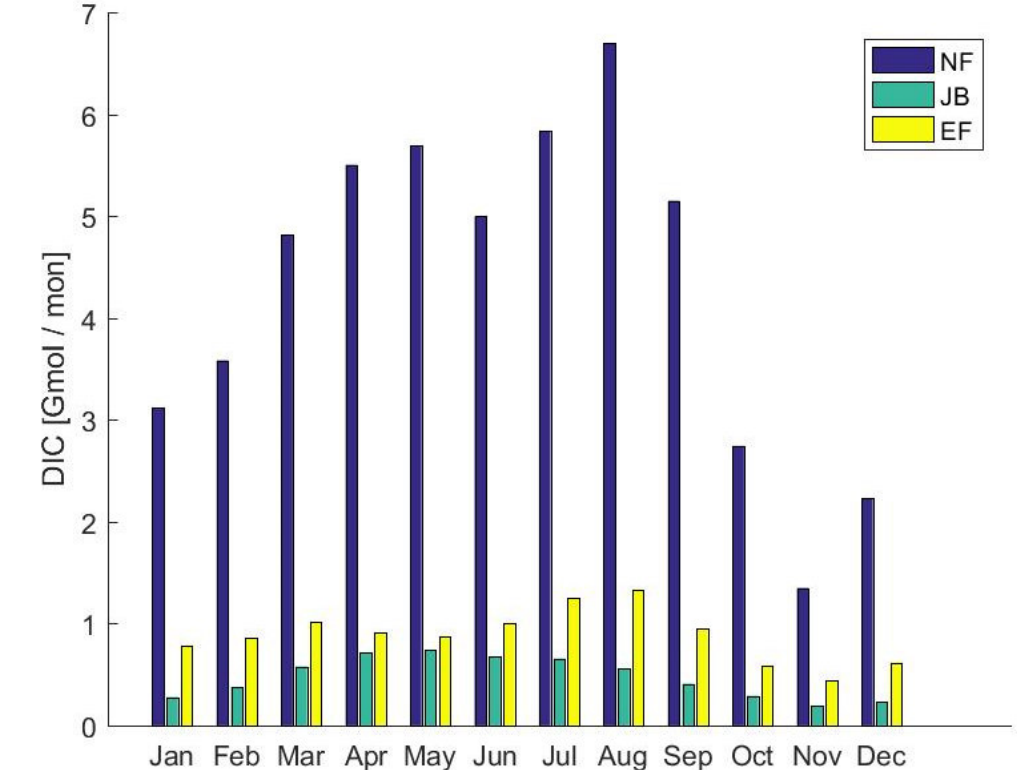


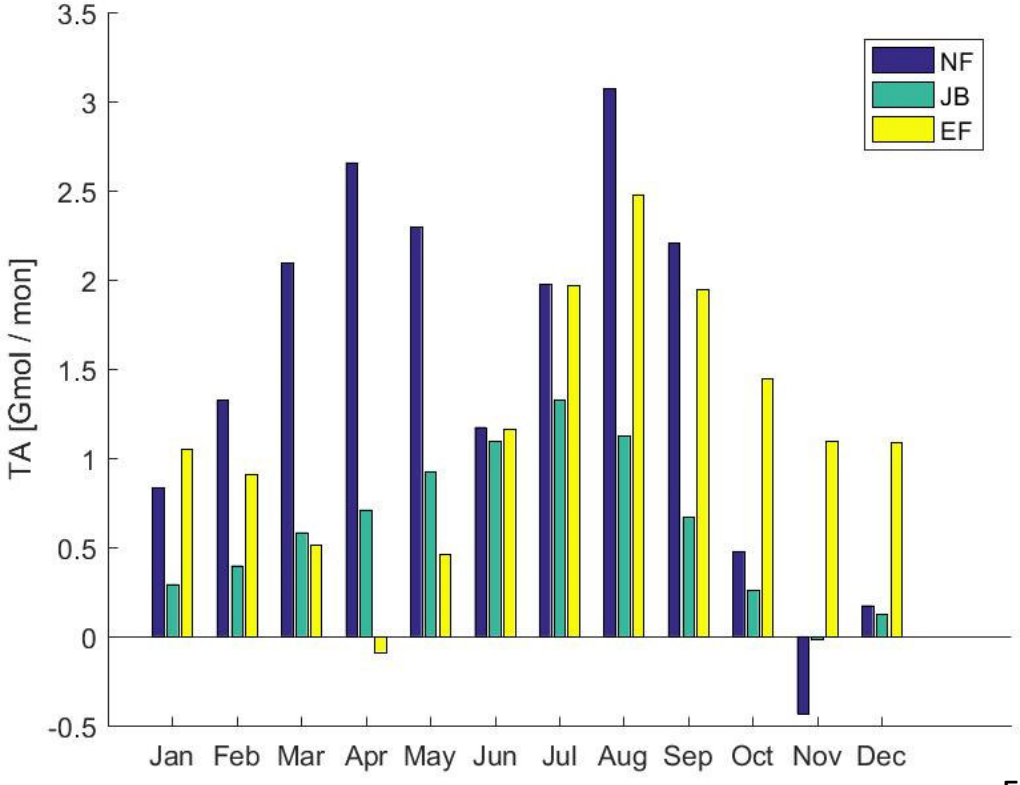


Fig. 2

https://doi.org/10.5194/bg-2020-24
Preprint. Discussion started: 29 January 2020


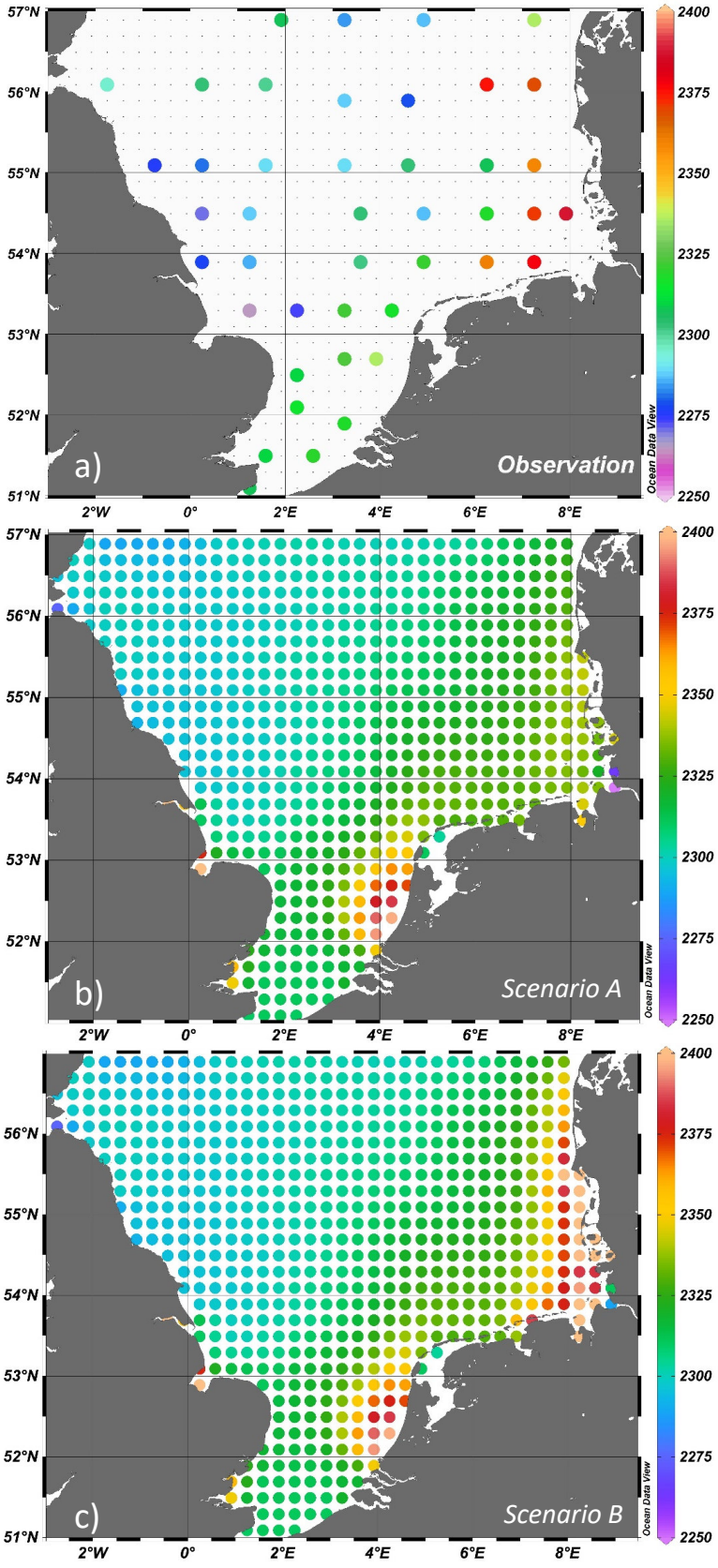


Fig. 3

https://doi.org/10.5194/bg-2020-24
Preprint. Discussion started: 29 January 2020


Biogeosciences
Discussions
Open Access
EGU

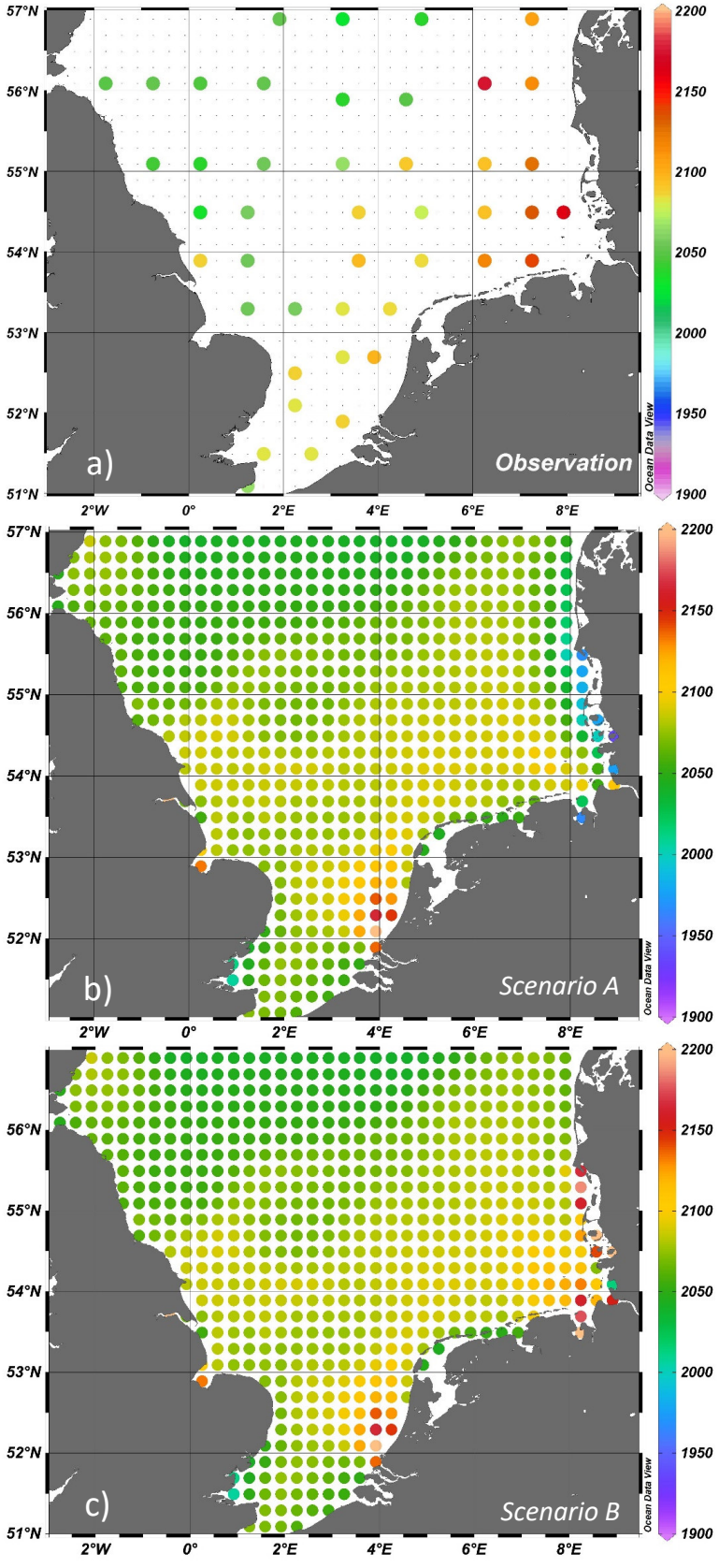


Fig. 4

https://doi.org/10.5194/bg-2020-24
Preprint. Discussion started: 29 January 2020


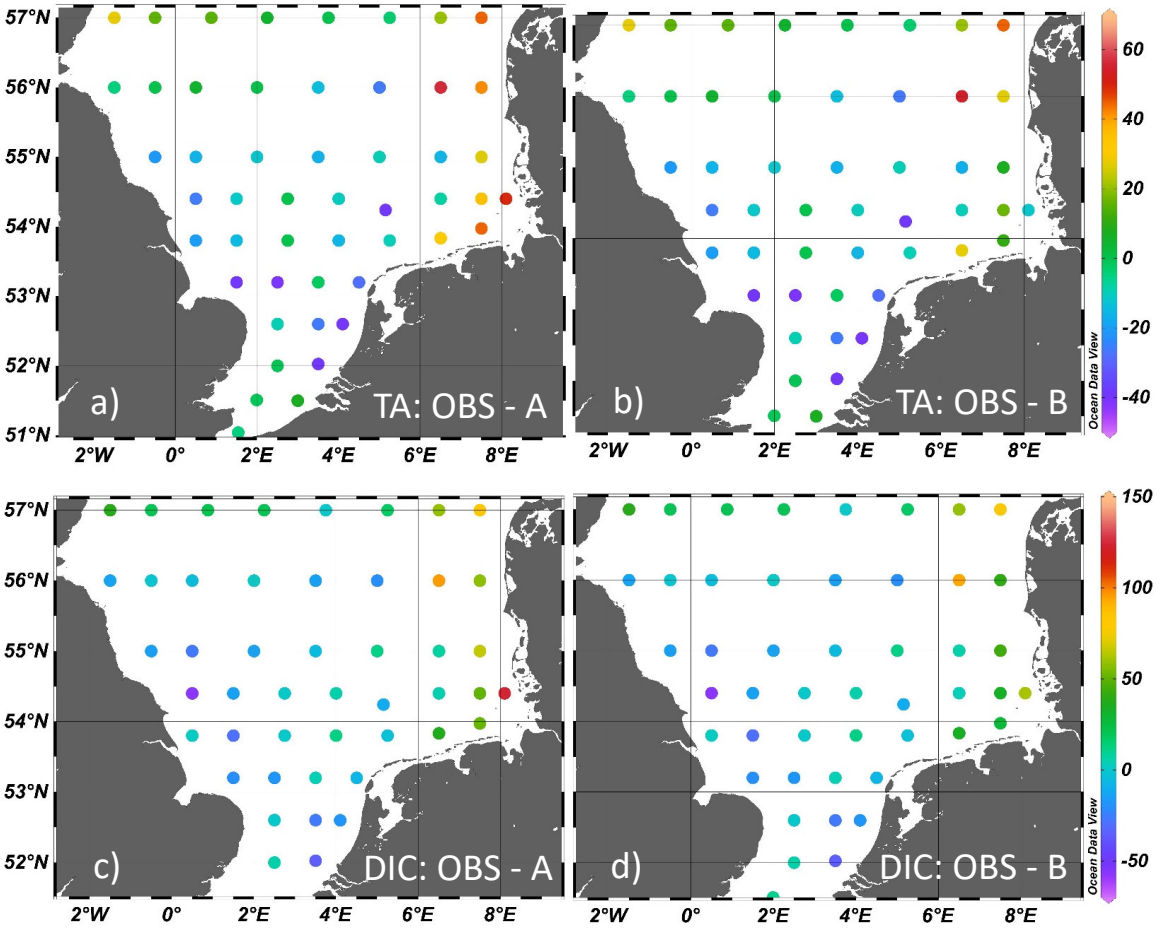


Fig. 5

https://doi.org/10.5194/bg-2020-24
Preprint. Discussion started: 29 January 2020


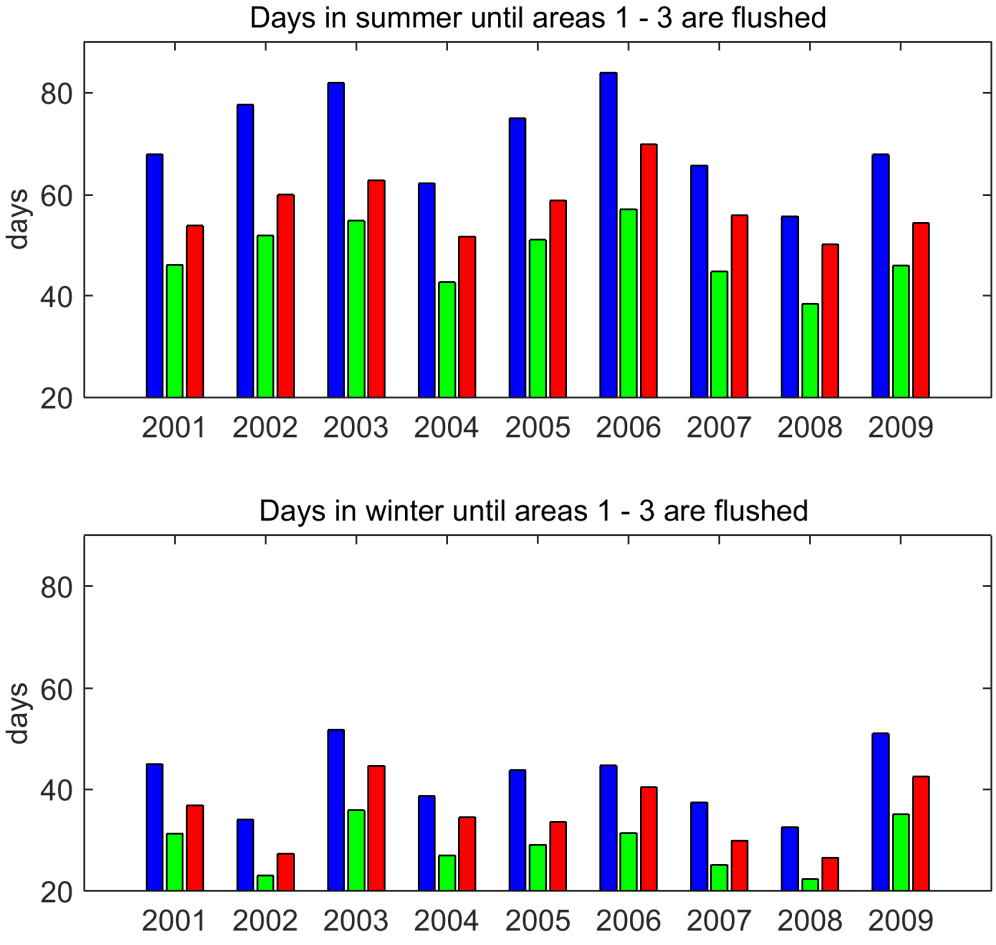


Fig. 6

https://doi.org/10.5194/bg-2020-24
Preprint. Discussion started: 29 January 2020


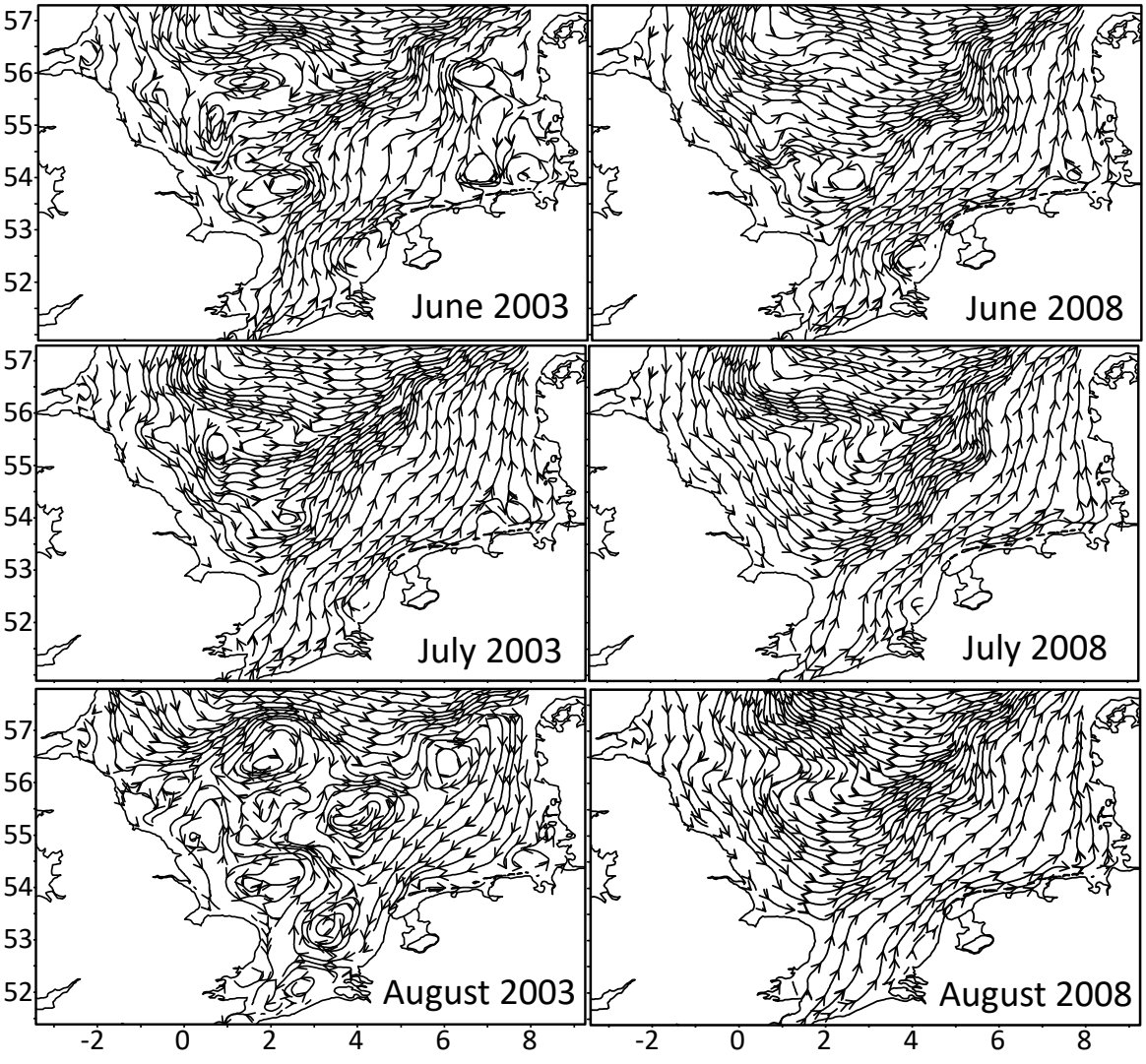


Fig. 7

https://doi.org/10.5194/bg-2020-24
Preprint. Discussion started: 29 January 2020


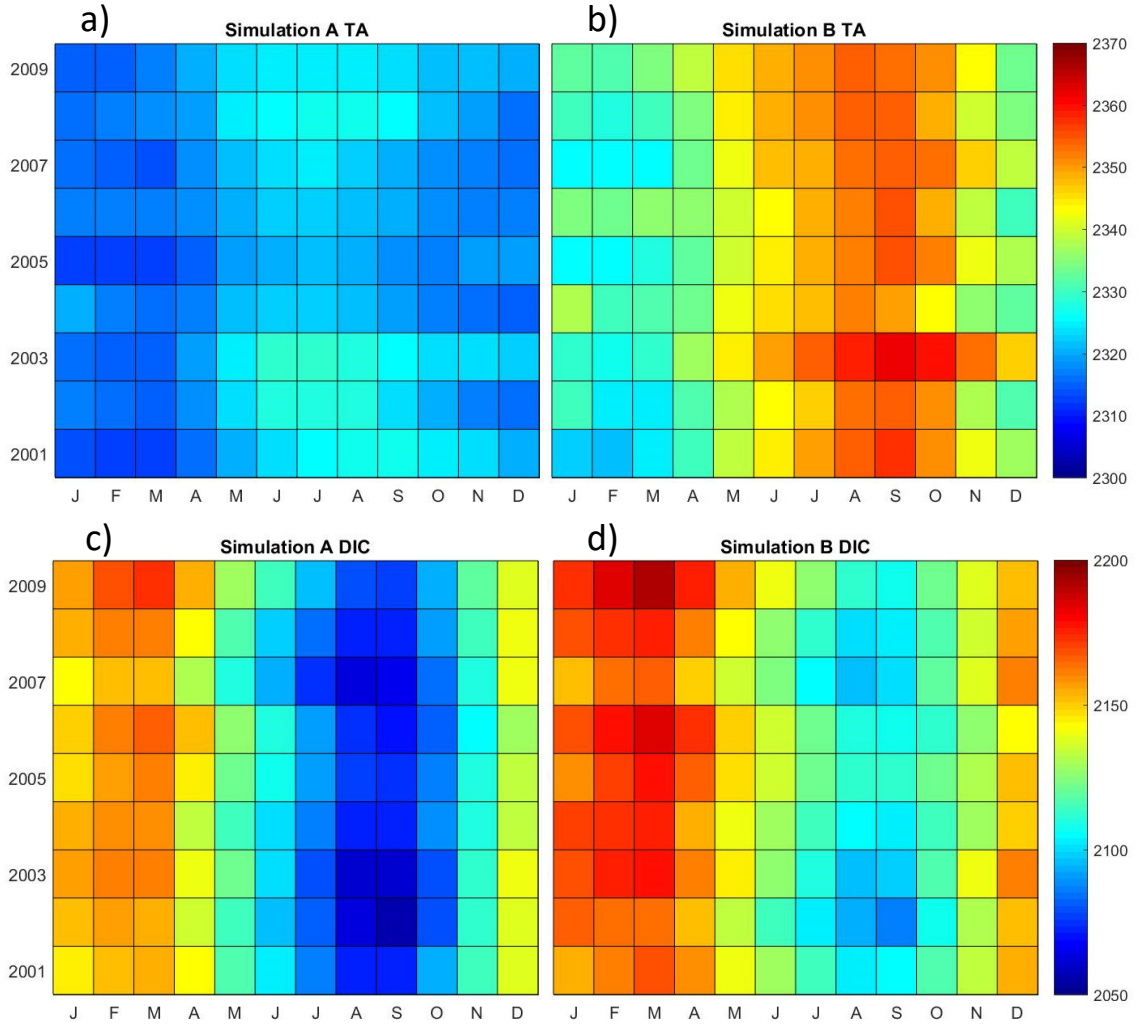


Fig. 8

https://doi.org/10.5194/bg-2020-24
Preprint. Discussion started: 29 January 2020


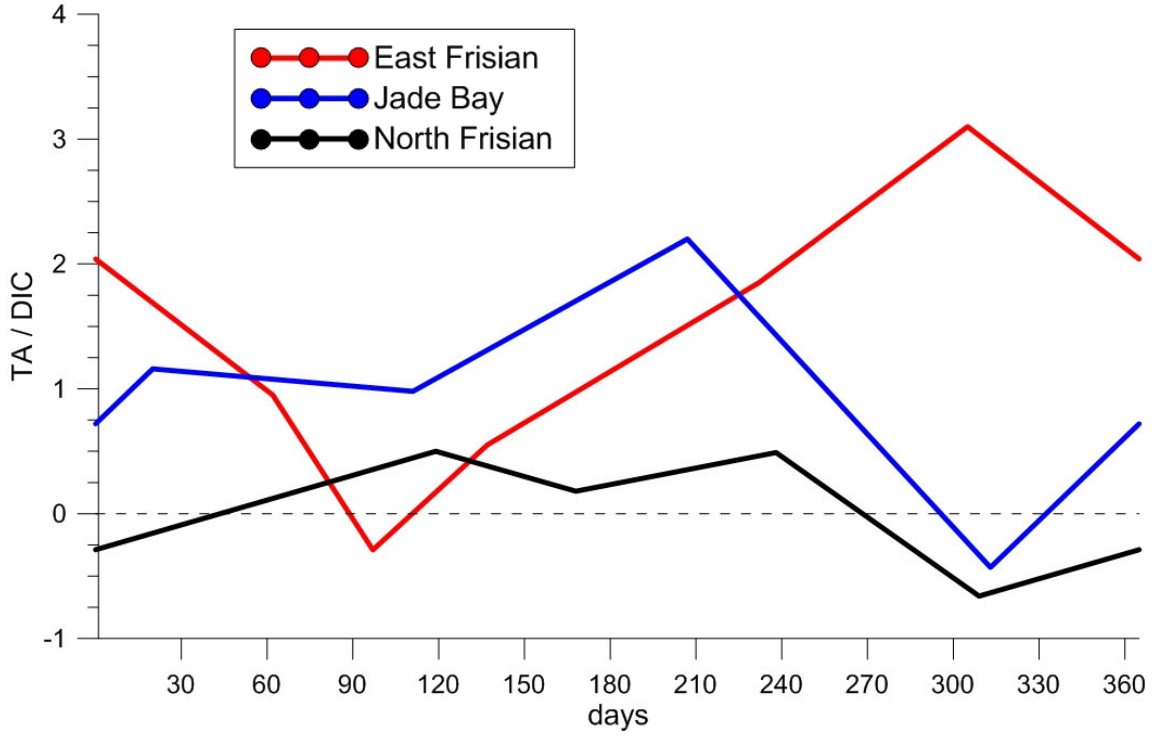


Fig. 9